JOURNAL OF COMPUTATIONAL PHYSICS **144,** 423–459 (1998)
ARTICLE NO. CP985993

Design Criteria for Local Euler Preconditioning

Dohyung Lee

Department of Aerospace Engineering, University of Michigan, Ann Arbor, Michigan 48109-2118
E-mail: dohyung@engin.umich.edu

Received May 21, 1997; revised December 31, 1997

Euler preconditioning has remarkable benefits in removing stiffness, making systems of equations behave as a scalar equation, preserving accuracy, and decoupling the Euler equations. Design criteria for optimal Euler preconditioning are discussed that retain the basic preconditioning benefits and remove the causes of instabilities due to the use of preconditioning. New families of 1D and 2D optimal Euler preconditioners are presented that may satisfy the design criteria in an optimal way. In particular, focusing on resolution of the stability problem associated with stagnation points, a stagnation preconditioner and a suboptimal Van Leer–Lee–Roe preconditioner are studied. These preconditioners are less sensitive to flow-angle variation across cells and/or produce a closer-to-orthogonal eigenvector system.

1. INTRODUCTION

The technique of time marching has become a popular method for solving steady-state problems in computational fluid dynamics. Its attraction is that it offers the freedom of changing the governing partial differential equations as long as the initial/boundary-value problem remains well posed and the steady solution is not affected. This freedom is no luxury, as the time-accurate systems of the Euler and Navier–Stokes equations may exhibit considerable stiffness, depending on the Mach and Reynolds numbers. For the Euler equations ($Re = \infty$), the degree of stiffness is measured by the *characteristic condition number*, which is the ratio of the largest to the smallest characteristic speed. In very slow ($M \downarrow 0$) or transonic flow ($M \approx 1$), the condition number increases without bound since the smallest speed approaches zero. This slows down the convergence speed of any time-marching method; in addition, for low Mach numbers standard discretizations lose their accuracy. In the Navier–Stokes equations, dissipative time-scales are added to the wave-propagation time-scales, creating more potential for stiffness.

The goal of *preconditioning* the equations is to equalize these embedded time-scales by changing the weights of the time-derivatives, thus making the equations better suited for efficient and accurate numerical approximation. The most general local preconditioning is

0021-9991/98 $25.00

achieved by multiplying the local vector of time-derivatives by a locally evaluated, positive-definite matrix. It changes the transient properties of the time-dependent solution, without affecting the final steady-state solution of the equations. This, at least, is true on the level of the partial differential equations. Preconditioning of the discretized equations may be done in a way that does affect the discrete steady solution; this may actually be advantageous with regard to stability and accuracy, as will appear later.

Chorin's method [3] of artificial compressibility for the incompressible Euler equations may be regarded as the the oldest contribution to the field. Starting from Chorin's method, Turkel [27–29] developed a two-parameter preconditioning matrix, of which the preconditioning benefit is limited to the low Mach-number range. Merkle *et al.* demonstrated significant convergence acceleration at low Mach numbers with a Euler preconditioner closely related to the Chorin–Turkel family [16, 33] and later extended to the Navier–Stokes equations. The only early preconditioners designed to have an effect over the entire Mach-number range are those in Viviand's four-parameter family [34]. These, however, are inspired by the isoenthalpic form of the Euler equations and do not have removal of stiffness as their goal.

More recently, Van Leer, Lee, and Roe [31, 14], by searching a multi-parameter family, derived an optimal preconditioning for the Euler equations, that is, one that achieves the lowest possible characteristic condition number over the entire Mach-number range. They demonstrated that the minimal achievable condition number deteriorates from unity in one space dimension to $1/\sqrt{1 - \min(M^2, M^{-2})}$ in three dimensions. When combined with an appropriate spatial discretization, the optimal preconditioning matrix yields the expected convergence acceleration over a wide range of Mach numbers, while it manages to preserve the solution accuracy at low Mach numbers. Another contribution by these authors is the development of a design tool linking the physics of wave propagation in a fluid to the numerical analysis. This is described in detail in Wen-Tzong Lee's Ph.D. thesis [14]. Using this tool, it is possible, for instance, to extend Turkel's matrix so that it is optimal for all Mach numbers [14].

One of the many remarkable benefits of an optimal preconditioning matrix is its ability to make the system of Euler equations, whether differential or discretized, behave more like a scalar equation. This property enables the development of explicit, multi-stage, time-marching schemes that efficiently damp all high-frequency error modes, as desired in multigrid relaxation. The Ph.D. theses of Chang-Hsien Tai [26] and John Lynn [15] are devoted to this subject.

Recently, it was discovered that the Van Leer–Lee–Roe preconditioning provides precisely the kind of decoupling of the Euler equations needed to accurately and efficiently apply multi-dimensional fluctuation-splitting schemes. An extensive account of this development is contained in the Ph.D. thesis of Lisa Mesaros [17].

As to local preconditioning for the Navier–Stokes equations, the research findings are more recent and more limited in number. Venkateswaran *et al.* [33, 2] have contributed a valuable method of analysis by which the proper dependence of the preconditioning on the Reynolds number can be determined. Godfrey *et al.* [10, 9, 7] circumvented the use of such an analysis by composing a Navier–Stokes preconditioner from the optimal Euler preconditioner and the Jacobi block for the discretized viscous/conductive terms.

Finally, Allmaras [1] and Pierce and Giles [21] consider pure block-Jacobi preconditioning for the discretized Navier–Stokes equations, equivalent to using block-Jacobi relaxation. This type of preconditioning always provides good high-frequency damping, which

is desirable for multigrid relaxation, but does not reduce the condition number, nor does it help preserve accuracy.

However, the numerical practices of these preconditioners show that different preconditioners producing the same optimal wave pattern lead to strongly different convergence histories. Since the wave patterns depend solely on the eigenvalues of the traveling wave solution, this outcome indicates the importance of the other properties of the preconditioned system such as corresponding eigenvectors. Lack of symmetrizability and positivity of certain preconditioned systems can become an issue, since these are associated with solution stability. When exploring the entire family of optimal preconditioners it therefore is important to be guided by a *healthy* eigenvector structure, i.e., not strongly deviating from orthogonality, and the symmetrizability of the preconditioned system, as well as other criteria which will be discussed in detail.

One of the major problems plaguing Euler preconditioners is that they usually lose robustness around a stagnation point. This is due in part to eigenvector degeneration, as shown by Darmofal and Schmid [4], and in part to the sensitivity of the preconditioned system to the flow angle, which is ill-defined near a stagnation point. Another phenomenon associated with the use of preconditioning is the generation of high transient vorticity near a stagnation point.

The detailed analysis of Euler preconditioners and the instability around the stagnation point is the purpose of this study. Some design criteria for more effective preconditioning and a preconditioner family, which satisfies the previous criteria in an optimal way, will be presented. Furthermore, some causes of instabilites at stagnation points and corresponding remedies will be shown. The design of Navier–Stokes preconditioners will be presented in a sequel paper [14a].

2. BASICS OF EULER PRECONDITIONING

A quasi-linear form of the Euler equations is expressed as

$$\mathbf{U}_t + \mathbf{A}\mathbf{U}_x + \mathbf{B}\mathbf{U}_y + \mathbf{C}\mathbf{U}_z = 0, \tag{1}$$

and a symmetric quasi-linear form is much favored for this analysis. For this purpose the symmetrization indicated by Turkel is attractive, as the state quantities are simple and the three coefficient matrices become equally sparse. Thus, we define

$$d\mathbf{U} = \begin{pmatrix} \frac{dp}{\rho a} \\ du \\ dv \\ dw \\ dp - a^2 d\rho \end{pmatrix}, \tag{2}$$

where a denotes the speed of sound; note that the fifth component is proportional to the

differential of entropy. The corresponding coefficient matrices are

$$\mathbf{A} = \begin{pmatrix} u & a & 0 & 0 & 0 \\ a & u & 0 & 0 & 0 \\ 0 & 0 & u & 0 & 0 \\ 0 & 0 & 0 & u & 0 \\ 0 & 0 & 0 & 0 & u \end{pmatrix}, \quad \mathbf{B} = \begin{pmatrix} v & 0 & a & 0 & 0 \\ 0 & v & 0 & 0 & 0 \\ a & 0 & v & 0 & 0 \\ 0 & 0 & 0 & v & 0 \\ 0 & 0 & 0 & 0 & v \end{pmatrix}, \quad \mathbf{C} = \begin{pmatrix} w & 0 & 0 & a & 0 \\ 0 & w & 0 & 0 & 0 \\ 0 & 0 & w & 0 & 0 \\ a & 0 & 0 & w & 0 \\ 0 & 0 & 0 & 0 & w \end{pmatrix}. \tag{3}$$

The analysis can be simplified even more by assuming that the flow is in the positive x-direction as v and w vanish and u becomes the full flow speed.

Wave propagation according to the Euler equations can be explored by inserting a plane-wave solution propagating in the direction of some unit vector $\hat{\mathbf{n}}$. Equation (1) reduces to

$$\hat{\mathbf{U}}_t + \mathbf{A}_n \hat{\mathbf{U}}_n = 0, \tag{4}$$

with

$$\mathbf{A}_n = (\mathbf{A}, \mathbf{B}, \mathbf{C}) \cdot \hat{\mathbf{n}} = \mathbf{A}n_x + \mathbf{B}n_y + \mathbf{C}n_z. \tag{5}$$

The propagation speeds in this direction are the eigenvalues λ_k of $\mathbf{A}_n$,

$$\lambda_1 = \vec{\mathbf{q}} \cdot \hat{\mathbf{n}} - a, \qquad \lambda_{2,3,4} = \vec{\mathbf{q}} \cdot \hat{\mathbf{n}}, \qquad \lambda_5 = \vec{\mathbf{q}} \cdot \hat{\mathbf{n}} + a; \tag{6}$$

here $\vec{\mathbf{q}}$ is the flow-speed vector, with magnitude q. In practice, however, it is more useful to consider the propagation of a point disturbance. Using a lesser known variant of Huygens' principle, which says that the wave front created by a point disturbance is the envelope of all plane-wave fronts that passed simultaneously through that point, we can determine the shape of the front from (6).

Figure 1 shows wave propagation of 2D Euler equations at $M = 0.5$; the circles indicate the plane-wave speeds created by a point disturbance and the dashed lines are all plane-wave fronts, of which envelopes are physical wave fronts. A point disturbance in entropy or vorticity remains a point propagating at the flow speed, while an acoustic disturbance becomes a circle centered at that point with radius, a.

Figure 1 also illustrates that, for any Mach number, the fastest and the slowest waves are always moving in the flow direction. For the Euler equations, the *condition number* is simply defined as the ratio between the largest and smallest wave speeds. It is sometimes called the *characteristic condition number*, in reference to the characteristic speeds of the Euler system of equations. The mathematical expression for the *condition number* of a matrix $\mathbf{A}$ is

$$K(\mathbf{A}) = \frac{|\lambda|_{max}}{|\lambda|_{min}}, \tag{7}$$

where $|\lambda|_{max}$ and $|\lambda|_{min}$ are the largest and smallest absolute eigenvalues of matrix $\mathbf{A}$.

The characteristic condition number determines the stiffness of the system of equations when marching in time. With explicit local time-stepping, the allowable local time step is limited by the fastest moving wave, since it must satisfy the CFL condition. During such a

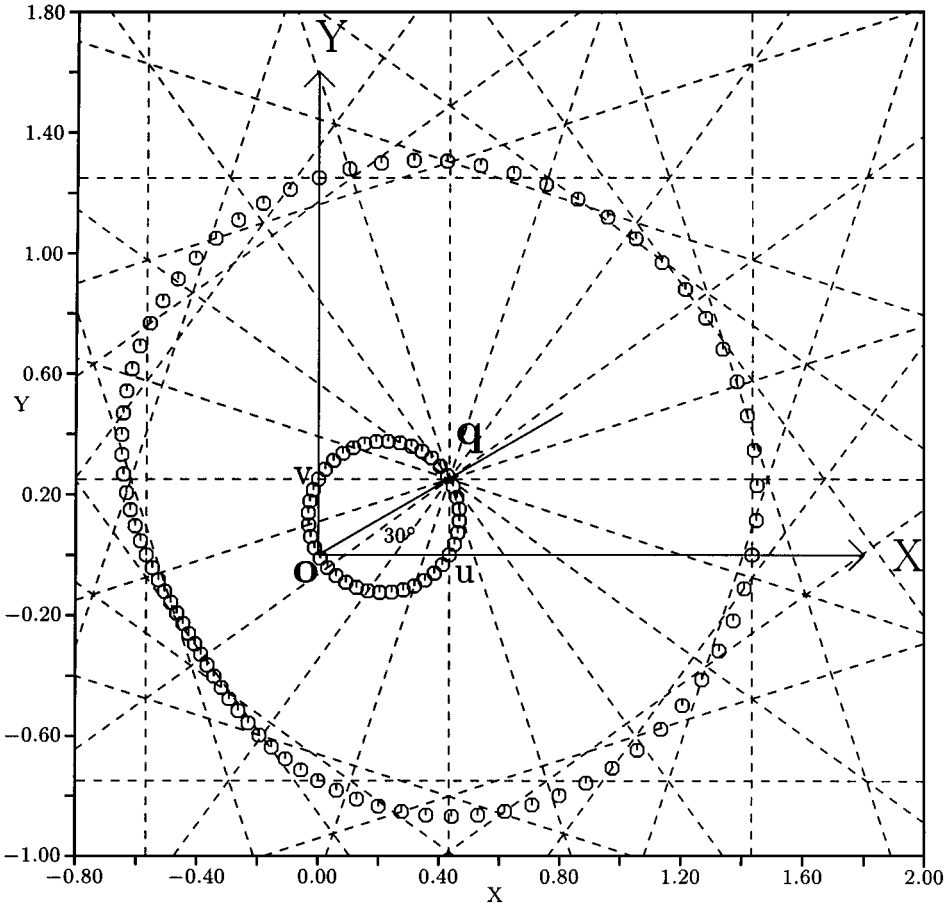

FIG. 1. Polar plot of plane-wave speeds (circle symbols) and the corresponding plane-wave fronts (dashed lines) for the Euler equations without preconditioning; $M = 0.5$, flow angle $= 30^\circ$. (NB. The plane-wave fronts are drawn only for every fourth point, otherwise the plot would become too crowded with wave-front lines.)

time step the slowest wave moves only over a fraction of the mesh width,

$$|\lambda|_{min}\Delta t = \frac{|\lambda|_{min}}{|\lambda|_{max}}h = \frac{h}{K(\mathbf{A})}, \tag{8}$$

where h is some representative mesh width; note that the condition number appears in the denominator. Thus a large condition number reduces the efficiency of wave propagation, needed for convergence. This remains true, to a lesser degree, for an implicit scheme, because of time-step limitations related to approximate factorization or approximate inversions of a time implicit operator.

Figure 2 shows the condition number for these regimes, indicating that the stiffness of the original Euler equations increases beyond bound as the Mach number approaches 0 or 1. This implies that, in fighting stiffness, preconditioning should focus on these incompressible and transonic flow regions.

Minimizing the characteristic condition number means minimizing the spread among the wave speeds, and therefore, increasing the efficiency of the wave-propagation mechanism.

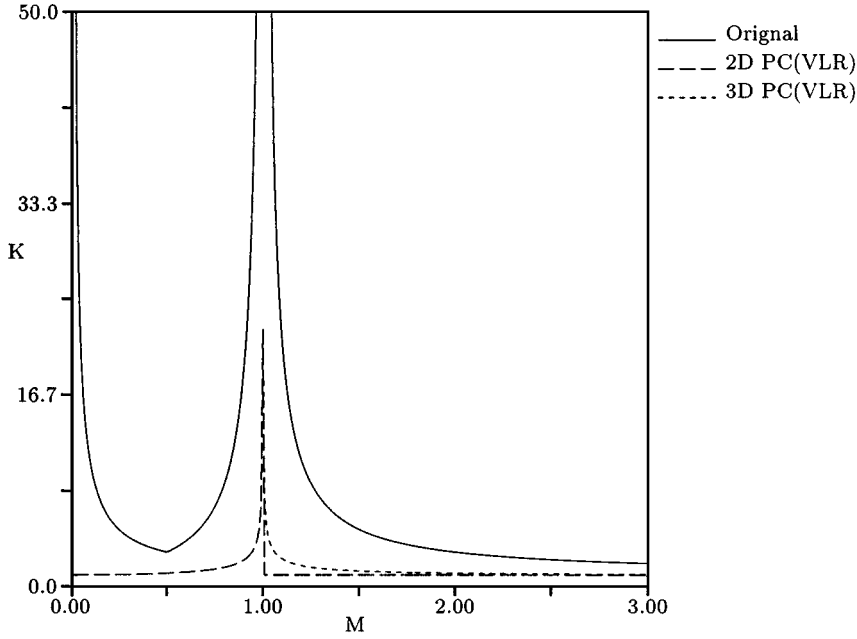

FIG. 2. Condition number for the Euler equations where 2D PC is the condition number after optimal 2D preconditioning; 3D PC is the condition number after optimal 3D preconditioning. In 1D (not shown), perfect preconditioning ($K = 1$) is possible for all Mach numbers.

The preconditioned system of equations thus becomes

$$\mathbf{P}^{-1}\mathbf{U}_t + \mathbf{A}\mathbf{U}_x + \mathbf{B}\mathbf{U}_y + \mathbf{C}\mathbf{U}_z = 0, \tag{9}$$

or

$$\mathbf{U}_t + \mathbf{P}(\mathbf{A}\mathbf{U}_x + \mathbf{B}\mathbf{U}_y + \mathbf{C}\mathbf{U}_z) = 0, \tag{10}$$

where $\mathbf{P}$ is the locally evaluated preconditioning matrix. The goal of preconditioning is to make the envelope of the plane waves coincide as much as possible with a sphere centered at the origin, for all possible Mach numbers and flow angles; in the preconditioning case, wave speeds are decided by $\mathbf{P}\mathbf{A}_n$, instead of $\mathbf{A}_n$, in Eq. (5).

Using the wave-propagation analysis of the previous subsection, Lee, Van Leer, and Roe [31, 14] developed an optimal symmetric preconditioner,

$$\mathbf{P}_{\mathrm{VLR}} = \begin{pmatrix} \frac{\tau}{\beta^2}M^2 & -\frac{\tau}{\beta^2}M & 0 & 0 & 0 \\ -\frac{\tau}{\beta^2}M & \frac{\tau}{\beta^2}+1 & 0 & 0 & 0 \\ 0 & 0 & \tau & 0 & 0 \\ 0 & 0 & 0 & \tau & 0 \\ 0 & 0 & 0 & 0 & 1 \end{pmatrix}, \tag{11}$$

where $\beta = \sqrt{|1 - M^2|}$ and $\tau = \min(\beta, \beta/M) = \sqrt{1 - \min(M^2, M^{-2})}$. This preconditioning matrix achieves an optimal reduction of the 3D Euler condition number to

$1/\sqrt{1-\min(M^2, M^{-2})}$, as seen in Fig. 2. The convergence efficiency is enhanced most by reduction of the condition number down to a perfect value of one at very low Mach numbers. Even at the transonic region, the condition number is much smaller than in the unpreconditioned case. However, 2D Euler preconditioning allows perfect conditioning ($K = 1$) for supersonic flow; in subsonic flow, the condition number is the same as in the 3D case.

3. BENEFITS OF EULER PRECONDITIONING

The basic goal of preconditioning is to reduce the stiffness of the system of equations, which, in turn, results in convergence acceleration for time-marching methods. This, though, is not the only possible benefit of preconditioning.

Below we list all major benefits that so far have come to light in the development of optimal local Euler preconditioning.

(1) *Removal of stiffness.* Local preconditioning can remove or reduce the stiffness of the system of Euler equations caused by the range of the characteristic speeds, thus improving the convergence rate of any discrete marching scheme [31]. In the nearly incompressible regime the stiffness can be entirely removed; in the transonic regime, it can be substantially reduced. In numerical practice, the condition number becomes a function of the aspect ratio(s) of the computational cell; in consequence, multidimensional preconditioners must include aspect-ratio dependence.

(2) *System behaves as a scalar equation.* Preconditioning makes the system of Euler equations behave more like a scalar equation, because the spread among the eigenvalues is removed or reduced. This is also true for discretizations of the Euler equations. This property is advantageous in designing and applying additional convergence-acceleration techniques such as multi-stage marching schemes with optimal high-frequency damping, and residual smoothing. Other techniques that may benefit are GMRES [35, 22], because of the local clustering of eigenvalues, and approximate factorization, owing to a reduction of the factorization error.

(3) *Accuracy preservation for $M \to 0$.* The accuracy of the discretization can be improved by preconditioning if the artificial viscosity term is modified[1] accordingly. In particular, the preconditioned equations retain the accuracy at a very low Mach number. This is achieved by properly balancing the artificial-viscosity term with the inviscid flux term. Without preconditioning, standard upwind and other schemes have an amount of artificial viscosity that does not scale correctly for $M \to 0$, and the accuracy deteriorates.

(4) *Decoupling of Euler equations.* The Van Leer–Lee–Roe, Turkel, and other preconditionings have the property of being able to decouple the entropy advection equation from the Euler equations. Moreover the Van Leer preconditioner allows perfect decoupling of the system of 2D Euler equations into an acoustic and an advective part (both enthalpy and entropy modes): in 2D the acoustic system only involves derivatives of p and v. Such decoupling allows the development of genuinely multidimensional discretizations [18, 17, 19, 20, 6, 5, 23, 24], as demonstrated by Roe (University of Michigan) and Deconinck (Von Karman Institute, Belgium) and their students.

[1] The modification was found to be needed in the first place to lift an unusually severe restriction on the time-step [14, 31].

4. DESIGN CRITERIA OF EULER PRECONDITIONING

As explained in the previous section, preconditioning provides many important advantages on both p.d.e. and the numerical scheme level. However, adopting an artificial technique in a numerical scheme may also produce unnecessary extra drawbacks. To maintain the advantages and to minimize the artificial disadvantages, it is important to construct a proper analytic preconditioner because the above characteristics are strongly related to the form of the preconditioner. Therefore, a list of design criteria for proper preconditioning is documented below to retain the above benefits and to remove the causes of instabilities due to preconditioning. Some of these design criteria must be definitely satisfied; others simply lead to an improved preconditioning performance.

(1) *Positivity.* The preconditioning matrix must be positive-definite, in order to agree with the boundary conditions that define the steady state. This criterion is fundamental, but does not restrict the choice of preconditioners very much. Moreover, a small violation appears to be allowed. For example, the unmodified stagnation preconditioner to be discussed is slightly non-positive but has been successful in computing stagnation flow.

(2) *Symmetrizability.* It is well known that a stable hyperbolic system of equations must possess a similarity transformation to a symmetric system [11]. Hyperbolic systems of conservation laws, such as the Euler equations and the equations of ideal magnetohydrodynamics, have this property; it also implies the existence of an extra entropy-conservation law [11, 12]. While the Van Leer–Lee–Roe preconditioner is already symmetric for the usual symmetrizing variables, other preconditioners such as Turkel's and D. Lee's stagnation preconditioner lie at the limit of system symmetrizability and need a slight modification to satisfy the symmetrizability condition. The symmetrizability is fundamental, although it, too, appears to tolerate small violations, and leaves much freedom of choice.

(3) *Reduction of spread among eigenvalues.* Reducing the spread among the eigenvalues of the Euler equations is the prime design criterion in developing preconditioners. Optimizing the condition number greatly reduces the choice of preconditioners, but still leaves enough parameters to achieve other goals. By allowing a slightly suboptimal condition number, the freedom may be usefully enlarged.

(4) *Decoupling into convective and acoustic equations.* The ability of the preconditioner to decouple the convective from the acoustic equations enables the implementation of genuinely multidimensional discretizations [18, 17], and the use of different, best suitable relaxation methods for the different types of equations [25]. There are different levels of decoupling that may be pursued. If we insist on keeping only derivatives of pressure and flow angles in the acoustic subsystem, the criterion is very restrictive: only the Van Leer–Lee–Roe preconditioner and a suboptimal variant of it [32] can achieve this. On the other hand, decoupling of the entropy equation only is a much less restrictive and still useful condition. More restrictive is the condition that one of the convected quantities must be the *total enthalpy*. By this criterion half of all optimal preconditioners must be discarded; these are the transpose of the admissible ones. In general, if attention is given to the criterion (3), reduction of eigenvalue speed, and (5), sparseness, the acoustic/convective decoupling will appear as a by-product.

(5) *Sparseness of preconditioner.* This criterion is related to the decoupling criterion. When trying to satisfy the various other criteria, we should look for the sparsest possible preconditioning matrix (using the symmetrizing variables) so as to avoid unnecessary coupling of the equations.

(6) *Clustering of numerical eigenvalues for all M.* Even when a preconditioner achieves the eigenvalue optimization on the p.d.e. level, the discretized preconditioned equations may fail to produce the expected eigenvalue clustering. Consideration of the Fourier footprint can, for instance, filter out incorrectly generalized preconditioners, previously known only for a small Mach number; this criterion is not very restrictive.

(7) *Proper balance between artificial dissipation and inviscid flux derivatives for* $M \to 0$. To preserve the accuracy of solutions in the incompressible limit, the artificial-viscosity and advection terms must scale similarly with M. This condition is not too restrictive; the explicit form of a preconditioner meeting this condition is known. The only widely used preconditioning known to violate this condition is Jacobi preconditioning, which also does not improve the condition number either.

(8) *Insensitivity to flow angle for* $M \to 0$. Preconditioners with a strong flow-angle dependence may fail to produce converged solutions, especially if stagnation regions are present. Insensitivity to the flow angle is desirable for stability and convergence. This condition is not too restrictive, as it seems to be important only for $M \to 0$.

(9) *Non-parallel eigenvector structure, especially for* $M \to 0$ *and* 1. Loss of orthogonality among eigenvectors can cause a transient amplification of error components, possibly leading to instability. Most preconditioners produce pairs of parallel eigenvectors as the Mach number approaches zero, but there appears to be a special class of optimal preconditioners, including D. Lee's stagnation preconditioner, that maintains a more nearly orthogonal eigenvector structure. Eigenvector degeneration may also occur at $M = 1$ or any other Mach number. This condition is quite restrictive, and one of the major concerns of current research.

(10) *Minimal artificial-vorticity production near a stagnation point.* To prevent numerical instability near a stagnation point, numerical vorticity production must be reduced. This condition is not so restrictive; an explicit recipe to prevent artificial vorticity production perfectly is developed by Roe [13].

(11) *Continuity at* $M = 1$. For a consistent preconditioning effect in the transonic regime, the subsonic and supersonic branches of the preconditioner must have a smooth connection, in some sense, at the sonic point, even though the matrix itself may be singular. This condition is strongly discriminating, and a valuable selection criterion.

5. ROBUSTNESS ISSUES

Though local preconditioning provides benefits such as convergence speed-up and accuracy improvement at low Mach number, these come at the expense of robustness. This section focuses on a more detailed issue: reliability of preconditioner around flow singularities such as stagnation points. The analysis for a general Euler preconditioner family and the overall design criteria will be discussed from 1D to 2D in the following Section 6.

One serious problem associated with the use of local preconditioning, even if it does the right thing in the limit of incompressibility, is that it commonly breaks down *locally* when the Mach number vanishes, i.e., in a stagnation point. It is evident that, for a preconditioner to be called reliable, it must achieve stability for stagnation flow, since most practical numerical problems have one or more local stagnation regions. In this section, we describe research on the loss of stability in computing stagnating flow with the symmetric Van Leer–Lee–Roe preconditioning [31], caused by flow-angle sensitivity, and how this sensitivity was reduced in two totally different ways: (a) by modifying the matrix (Subsection 5.2); (b) by developing

a completely new matrix with superior properties for low Mach numbers (Subsection 5.3). In particular, the second method (b) produces the so-called "stagnation preconditioner," which was a basis for the low-speed regime in constructing optimal preconditioners for all Mach numbers in Section 6.

5.1. *Instability in a Stagnation Region*

There are four reasons for the instability in a stagnation region.

(1) *Unstable local time step.* The first one is related to the small magnitude of the Mach number. As the Mach number decreases in a stagnation region, the allowable local time step for the preconditioned equations increases as $1/M$, varying strongly from cell to cell. It is easy to devise the preconditioned scheme unstable by local time-stepping; this type of instability can be prevented by putting a safety factor or a cap on the time step.

(2) *Degeneration of eigenvectors.* Furthermore, the small Mach number reduces the orthogonality between eigenvectors of the preconditioned matrix coefficients, increasing the chance of transient growth, since the eigenvector basis is not effectively spanning the space. This will happen for any value of the time step, and can be aggravated by large velocity and/or pressure perturbations arising in the stagnation region. This happens for instance when the calculation of flow over an airfoil is started "impulsively," i.e., with free-stream velocity everywhere. The perturbations near the stagnation point then are of the size $\rho_\infty u_\infty^2 \sim p_\infty M_\infty^2$, which is particularly large if M_∞ is not small [4].

(3) *Flow angle sensitivity.* The third reason comes from the fact that the flow angle varies substantially around the stagnation point, and the preconditioned equations may be over-sensitive to this variation.

(4) *Vorticity production.* In unpreconditioned Euler equations, vorticity is merely transported with the flow speed; the vorticity is produced only due to interference of an wall boundary or a shock. However, preconditioned p.d.e.'s may have artificial vorticity production terms, of which effect is exaggerated around the stagnation point where velocity and pressure fields vary substantially.

5.2. *Flow-Angle Sensitivity and How to Reduce It*

To explain the part of the stagnation instability that is due to the preconditioner's sensitivity to flow angle, we analyze the behavior of the Van Leer–Lee–Roe preconditioning matrix (11) for low Mach numbers. For subsonic flow ($\beta = \tau = \sqrt{1 - M^2}$), the matrix is expressed in generalized Cartesian coordinates as

$$\mathbf{P}_{\mathrm{VLR}\phi} = \begin{pmatrix} \frac{M^2}{\beta} & -\frac{M}{\beta}\cos\phi & -\frac{M}{\beta}\sin\phi & 0 \\ -\frac{M}{\beta}\cos\phi & \left(\frac{1}{\beta}+1\right)\cos^2\phi + \beta\sin^2\phi & \left(\frac{1}{\beta}+1-\beta\right)\sin\phi\cos\phi & 0 \\ -\frac{M}{\beta}\sin\phi & \left(\frac{1}{\beta}+1-\beta\right)\sin\phi\cos\phi & \left(\frac{1}{\beta}+1\right)\sin^2\phi + \beta\cos^2\phi & 0 \\ 0 & 0 & 0 & 1 \end{pmatrix}, \tag{12}$$

where ϕ is the flow angle. Considering this matrix, the pattern of flow-angle dependence among the matrix elements emerges as a possible source of trouble: the inner elements (2, 2), (2, 3), (3, 2), and (3, 3), which depend on ϕ, remain $\mathcal{O}(1)$ for $M \downarrow 0$, while the

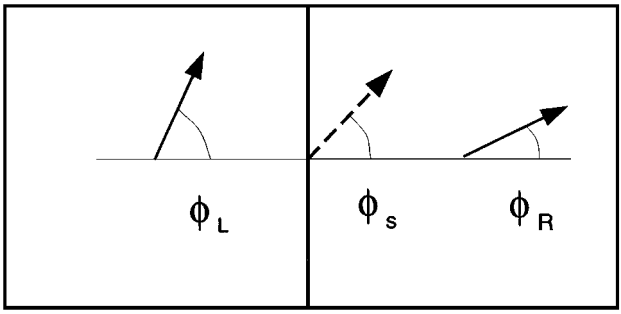

FIG. 3. Flow angle variation across cells.

remaining elements are $\mathcal{O}(M, M^2)$. This makes the preconditioning particularly sensitive to the flow angle when the Mach number approaches zero. In the case where u and v are small in absolute value, numerical perturbations may not be small compared to the values of u and v, causing $\mathcal{O}(1)$ variations in ϕ and, therefore, in the four matrix elements. This is believed to be at least one of the causes of numerical instability near a stagnation point, in particular, when experienced with a *conservative* upwind Euler scheme, associated with the use of the above preconditioning matrix. The sensitivity can be eliminated when the angle dependence is completely removed from the matrix elements, or it can be much reduced when only the quadratic terms in $\cos\phi$ and $\sin\phi$ are removed.

In a conservative upwind scheme, the flow angle sensitivity is emphasized in the preconditioned artificial-dissipation matrices [31], whose cell-face values become

$$\mathbf{P^{-1}}|\mathbf{PA}|, \qquad \mathbf{P^{-1}}|\mathbf{PB}|, \tag{13}$$

rather than $|\mathbf{A}|$ and $|\mathbf{B}|$, as in standard upwind schemes. In the update the spatial residual in each cell is multiplied by the cell-centered value of $\mathbf{P}_\phi$, creating products

$$(\mathbf{P}_\phi)_{\text{center}}\left(\mathbf{P}_\phi^{-1}\right)_{\text{face}} \tag{14}$$

that may vary erratically near a stagnation point and deviate appreciably from the values elsewhere in a smooth flow, which should be close to the identity matrix. If one simply ignores these products, replacing them by $\mathbf{I}$, the scheme becomes non-conservative and the sensitivity to ϕ reduces significantly. Figure 3 shows the sort of large flow-angle variations between the cell centers and interfaces that could cause the product (14) to differ appreciably from $\mathbf{I}$.

To further investigate the stagnation instability, a numerical study was performed as illustrated in Fig. 4. Figure 4(a) shows velocity vectors in uniform slow flow ($M = 0.1$) with an initial perturbation made by rotating the velocity over a certain angle in a single cell. Figure 4(b) is the uniform steady solution, obtainable without any preconditioning, or with a robust preconditioner. Note that the perturbation, although local, is not at all small, so linear stability theory does not offer any guarantee here. It turned out, for instance, that a 62° flow-angle rotation caused the solution to become unstable when advanced in time by an explicit first-order upwind scheme preconditioned by $\mathbf{P}_{\text{VLR}}$ with CFL number 0.7; see Table II. Using a smaller/larger CFL number will allow a larger/smaller angle-perturbation.

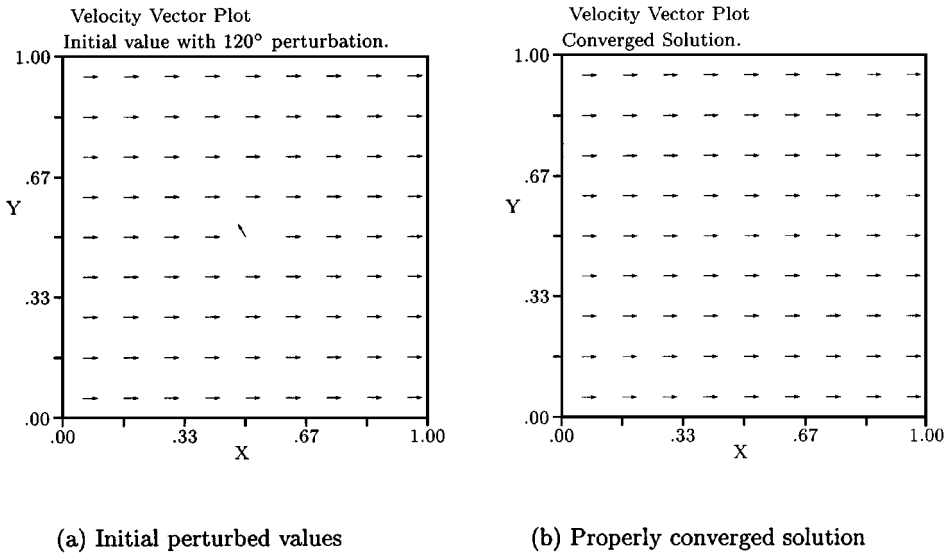

(a) Initial perturbed values (b) Properly converged solution

FIG. 4. Angle-perturbation test; $M = 0.1$.

The same scheme was also tested on a stagnation flow as shown in Fig. 5: the fluid is flowing from the top and bottom boundaries to the left and right boundaries. Without preconditioning the scheme reaches a reasonable-looking steady state (Fig. 5(a)). The instability from preconditioning is readily identified in Fig. 5(b) and appears to be due to totally wrong flow angles.

The stagnation instability could be forestalled, but not avoided, even by taking smaller time steps. Similar behavior was found when simulating subsonic flow over an airfoil at the leading-edge stagnation point. Godfrey reports that implicit time integration can suppress the instability if the grid used is not too fine [8].

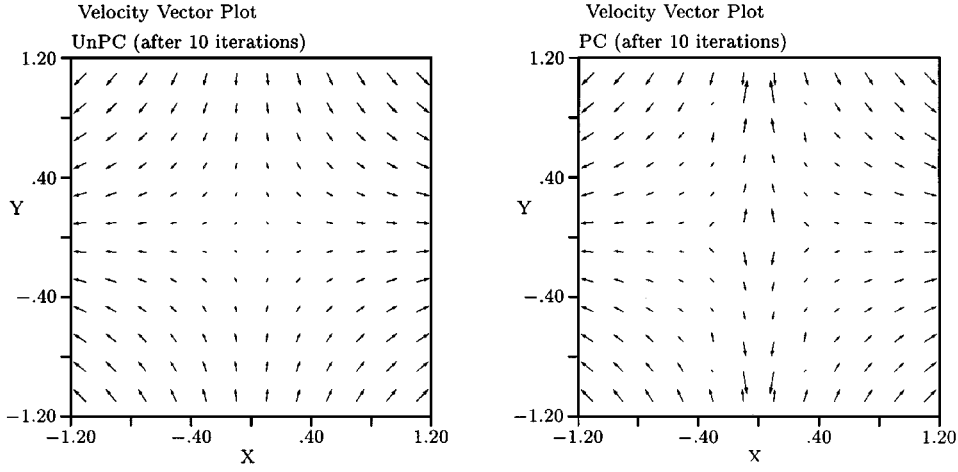

(a) Unpreconditioned. (b) Preconditioned ($\mathbf{P}_{VLR}$).

FIG. 5. Instability of stagnating flow; $M = 0.1$.

In contrast, it was reported by Tai [32] that schemes preconditioned by Turkel's preconditioning matrix (15), whether or not in conservation form, were less prone to the angle instability. This, in fact, was our motivation to examine and compare preconditioning matrices for arbitrary flow angle. The alleged greater robustness of Turkel's preconditioner can be understood from its structure. The Turkel matrix in 2D becomes

$$\mathbf{P_T} = \begin{pmatrix} \frac{M^2}{\beta} & 0 & 0 & 0 \\ -\frac{M}{\beta} & 1 & 0 & 0 \\ 0 & 0 & \beta & 0 \\ 0 & 0 & 0 & 1 \end{pmatrix}; \tag{15}$$

for low-speed flow along the x-axis Turkel's preconditioner reduces to

$$\mathbf{P_T} = \begin{pmatrix} M^2 & 0 & 0 & 0 \\ -M & 1 & 0 & 0 \\ 0 & 0 & 1 & 0 \\ 0 & 0 & 0 & 1 \end{pmatrix}. \tag{16}$$

Note that, unlike (12), this matrix has the property $P_{22} = P_{33}$, making the central block of the matrix invariant under rotation. For an arbitrary flow angle it becomes

$$\mathbf{P_{T\phi}} = \begin{pmatrix} M^2 & 0 & 0 & 0 \\ -M\cos\phi & 1 & 0 & 0 \\ -M\sin\phi & 0 & 1 & 0 \\ 0 & 0 & 0 & 1 \end{pmatrix}, \tag{17}$$

which is well behaved for $M \to 0$ since the flow-angle-dependent elements are $\mathcal{O}(M)$. The angle-perturbation test (Table II) shows that $\mathbf{P_T}$ will stand an angle perturbation up to 140°, regardless of the CFL number, which is much larger than the value for $\mathbf{P}_{\mathrm{VLR}}$. But it still fails to calculate the stagnation flow of Fig. 5, indicating there is an additional cause of stagnation instability.

It is not *a priori* clear that, in the limit of $M \to 0$, the matrix (16) is the only optimal preconditioner with the property that its (2, 2) and (3, 3) elements are equal. It would be preferable if an optimal matrix existed closer to Van Leer's, i.e., more nearly symmetric, in order to avoid losing symmetrizability; see Sections 6.1. Van Leer *et al.* [32] searched for reduced flow-angle sensitivity among all optimal 2D preconditioners of the form

$$\mathbf{P} = \begin{pmatrix} a & D & E & 0 \\ d & b & F & 0 \\ e & f & c & 0 \\ 0 & 0 & 0 & 1 \end{pmatrix}, \tag{18}$$

under the constraints $b = c$, $f = -F$, and proved there are none. Apparently, the extra freedom in the elements e, E, f, and F does not pay off. They therefore recommend to those wishing to stay within the family of optimal preconditioners to switch smoothly from

$\mathbf{P_T}$ to $\mathbf{P}_{\mathrm{VLR}}$ when varying M from 0 to 1. This idea is similar to the switching presented in Subsections 6.1 and 6.2, where the function $\zeta(M)$ is chosen to vary from $\zeta(0) = -1$ to $\zeta(1) = 1$.

The suboptimal symmetric preconditioner with the above idea becomes

$$\mathbf{P} = \begin{pmatrix} \alpha\frac{M^2}{\beta} & -\alpha\frac{M}{\beta} & 0 & 0 \\ -\alpha\frac{M}{\beta} & \alpha\left(\frac{1}{\beta}+1\right) & 0 & 0 \\ 0 & 0 & \beta & 0 \\ 0 & 0 & 0 & \alpha \end{pmatrix}, \tag{19}$$

where $\alpha(M)$ is the switch needed to link the sub-optimal matrix at $M = 0$ to the optimal form for $M > 0$. In the numerical experiments in [32], α was chosen as a blending of the form

$$\alpha = \frac{1}{2}, \qquad 0 \le M \le \frac{1}{3}, \tag{20}$$

$$\alpha = \frac{3}{4}\left\{1 + 3\left(M - \frac{1}{2}\right)\left[1 - 12\left(M - \frac{1}{2}\right)^2\right]\right\}, \qquad \frac{1}{3} < M < \frac{2}{3}, \tag{21}$$

$$\alpha = 1, \qquad \frac{2}{3} \le M \le 1, \tag{22}$$

which is a continuously differentiable function using a cubic to switch between the two plateau values. Note that another simpler switch function can be used for the value of α.

From numerical experiments performed with this matrix by Mesaros [32, 17], a striking result was obtained. The symmetric preconditioner greatly improved a *non-conservative* flow code, namely, the unstructured-grid code developed by Mesaros on the basis of fluctuation-splitting ideas. Previously, the fluctuation-split scheme failed to converge for flows around airfoils at low inflow Mach numbers, due to the leading-edge stagnation region. The sub-optimal symmetric preconditioner decoupled the equations just as the original optimal Van Leer preconditioner, and made it possible to achieve accurate converged results for arbitrarily low inflow Mach numbers on a fine grid. However, the conservative scheme still lost robustness for low-speed flows. Conservative solutions could be obtained only after the non-conservative scheme had handled the first transients.

5.3. *Complete Removal of Flow-Angle Dependence*

As shown in the previous section, the Van Leer–Lee–Roe preconditioning technique becomes unstable near a stagnation point. The instability was attributed in part to the incompatibility between $\mathbf{P}_{\mathrm{center}}$ and $\mathbf{P}_{\mathrm{face}}$ that appears in the artificial-viscosity flux. This incompatibility increases as flow-angle variations increase when the Mach number locally approaches zero as in a stagnation region. Therefore, one way to help prevent the instability problem is to remove the incompatibility to the extent possible.

A useful requirement to impose on $\mathbf{P}$ is that the product of itself and its inverse, evaluated at different neighboring locations, be close to the identity matrix. In the stagnation region, the flow-angle is changing rapidly; therefore, we must concentrate on reducing the flow-angle dependence in $\mathbf{P}$.

A *stagnation preconditioner* is hereby defined as a matrix that, without having any flow-angle dependence, generates the same optimal wave patterns as the Van Leer–Lee–Roe and Turkel preconditioners do. The general form of the subsonic *stagnation preconditioning matrix* ($b_0 = 0$) becomes

$$\mathbf{P}_{\text{stag}} = \begin{pmatrix} M^2 & \pm M\sqrt{1+M^2}\cos\psi & \pm M\sqrt{1+M^2}\sin\psi \\ \mp M\sqrt{1+M^2}\cos\psi & \sin^2\psi - M^2\cos^2\psi & -(1+M^2)\sin\psi\cos\psi \\ \mp M1 + M^2\sin\psi & -(1+M^2)\sin\psi\cos\psi & \cos^2\psi - M^2\sin^2\psi \end{pmatrix}, \tag{23}$$

where ψ is the hidden "principal angle" of the preconditioning matrix. Among the two choices of sign in the preconditioner, the one with the positive sign in element (1, 2) gives better convergence performance owing to a nearly orthogonal eigenvector structure, specifically for low Mach numbers and for streamwise-moving plane waves. The other choice produces an eigenvector structure with two identical acoustic eigenvectors for a certain pair of streamwise moving plane waves at low Mach number, which slows down convergence and may cause an instability.

Note that any value of ψ produces the same desirable optimal wave pattern. While this is true at the p.d.e.-level, or, equivalently, for low-frequency Fourier modes, the principal angle clearly shows up in the high-frequency modes of a discretization. It turns out that for best results, the principal angle must be set equal to the local flow angle, and this so-called *streamwise stagnation matrix* still has the best performance in a stagnation region.

When ψ is set equal to the local flow angle, and the latter is set to zero as usual in our analysis, the matrix becomes the following sparsest form of (24). This *streamwise stagnation matrix*, presumably suitable for computing stagnating flow, is expressed as

$$\mathbf{P}_{\text{stag,streamwise}} = \begin{pmatrix} M^2 & M\sqrt{1+M^2} & 0 & 0 \\ -M\sqrt{1+M^2} & (b_0-1)M^2 & 0 & 0 \\ 0 & 0 & 1 & 0 \\ 0 & 0 & 0 & 1 \end{pmatrix}, \tag{24}$$

where $b_0 = 0$ gives the optimal wave pattern for all $M < 1$, but $b_0 > 1$ is needed for positive definiteness of $\mathbf{P}$ and symmetrizability of the preconditioned equations. As discussed earlier, a proper preconditioning has to satisfy other criteria such as positive definiteness and symmetrizability. With regard to positivity $\mathbf{P}_{\text{stag,streamwise}}$ yields

$$x^T\mathbf{P}x = M^2x_1^2 + (b_0-1)M^2x_2^2 + x_3^2, \tag{25}$$

and therefore is positive definite only when $b_0 > 1$. The inequality $b_0 > 1$ also will satisfy the symmetrizability condition. The consequence of a nonzero b_0 is that it makes the acoustic wave front non-symmetric about the flow-normal axis, causing loss of optimality for larger values of M.

The eigenvector structure of $\mathbf{P}_{\text{stag,streamwise}}$ is much more closely orthogonal than that of $\mathbf{P}_{\text{VLR}}$. Recall that, for $\mathbf{P}_{\text{VLR}}$, the enthalpy-convection eigenvector eventually collapses onto an acoustic eigenvector at very low Mach number. In contrast, $\mathbf{P}_{\text{stag,streamwise}}$ does not cause extreme departure from orthogonality.

With $\mathbf{P}_{\text{stag,streamwise}}$, the right eigenvectors for the waves traveling in the streamwise direction become

$$\mathbf{R}_1 = \begin{pmatrix} 1 \\ -M - M^5/12 \\ 0 \\ 0 \end{pmatrix} \approx \begin{pmatrix} 1 \\ 0 \\ 0 \\ 0 \end{pmatrix}, \qquad \mathbf{R}_2 = \begin{pmatrix} 0 \\ 0 \\ 1 \\ 0 \end{pmatrix},$$

$$\mathbf{R}_3 = \begin{pmatrix} M \\ -1 - M^3/2 - M^4/8 \\ 0 \\ 0 \end{pmatrix} \approx \begin{pmatrix} 0 \\ -1 \\ 0 \\ 0 \end{pmatrix}, \qquad \mathbf{R}_4 = \begin{pmatrix} 0 \\ 0 \\ 0 \\ 1 \end{pmatrix}, \tag{26}$$

as the Mach number approaches zero. The $\mathbf{R}_k$ represent eigenvectors, corresponding to forward and backward acoustics, enthalpy and entropy waves, in sequence.

Just as its simplified form studied in Subsections 6.1 and 6.2, this preconditioner preserves eigenvector orthogonality for waves moving in the streamwise direction, in the incompressible limit. A similar study for the eigenvectors of waves moving in the normal to the flow direction shows that the eigenvectors can be kept from moving too far away from orthogonality: the eigenvectors do not make angles $\leq 45^\circ$ (or $\geq 135^\circ$) with each other.

When performing a Fourier analysis of a difference scheme, properties at the p.d.e. level show up as properties of low-frequency modes. Wave-speed equalization and flow-angle insensitivity, such as obtained for the stagnation preconditioner, will thus be found for low-frequency modes. The behavior of high-frequency modes, which do not follow the p.d.e. accurately, may be totally different and, in fact, undesirable. To check the numerical propagation and damping produced by the first-order upwind spatial operator for all waves from low to high frequencies, a Fourier footprint (FFP) is produced for $\mathbf{P}_{\text{stag}}$. Figure 6 shows the FFPs resulting when varying the difference between the preconditioner's principal angle and the actual flow angle. When the angle difference is zero, the shape of the FFP is the same as that of the original Van Leer preconditioning. However, as the angle difference increases, the shape of the FFP changes to a less orderly pattern in which some high frequency eigenvalues cross the real axis, i.e., change sign in their imaginary part value. This means that high-frequency waves may propagate in a direction opposite to that of low-frequency waves, especially as the angle difference approaches 90°.

If the principal angle is set to a certain fixed global angle and the angle difference with the flow direction is too different, the high-frequency eigenvalues still may cause an instability, in spite of the insensitivity of the low-frequency eigenvalues to the angle difference. Therefore, preconditioning regardless of the flow angle remains a fiction. However, $\mathbf{P}_{\text{stag,streamwise}}$ ($\psi = \phi$) does a good job in stabilizing against the angle instability.

6. EULER PRECONDITIONER FAMILY

The design criteria in Section 4 cannot be satisfied by the same preconditioner, especially in multidimensions; i.e., there is no preconditioner that meets all the above conditions. For instance, reducing the sensitivity to the flow angle in the symmetric Van Leer–Lee–Roe preconditioner leads to either a loss of optimality [32] or loss of symmetrizability. Table I shows how the currently popular preconditioners score in each criteria; as can be seen, there

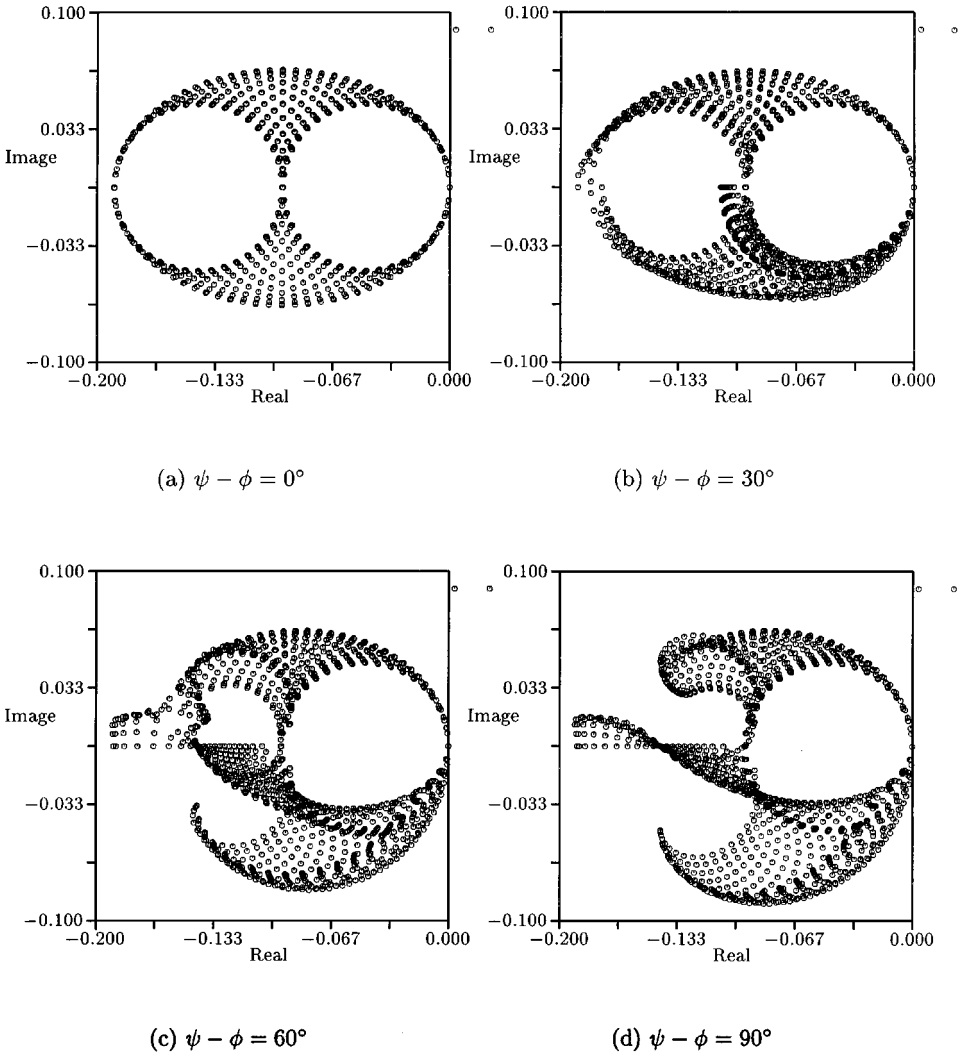

FIG. 6. Fourier Footprint for the first-order upwind spatial operator with stagnation preconditioner. The angle $\psi - \phi$ is the angle difference between the preconditioner's principal angle and the actual flow angle. $M = 0.1$.

is no preconditioner that meets all criteria. Therefore, a particular philosophy and overall understanding of each feature need to be discussed regarding the use of these criteria.

Among the criteria, positivity (1) and symmetrizability (2) must surely be satisfied to secure basic well-posedness and stability of the equation system; this is usually verified after the choice of preconditioners has been substantially narrowed down. Eigenvalue optimization (3), while keeping the matrix sparse (5), is the single most important criterion for reducing the vast number of possibilities to an manageable subset. At this point, decoupling (4) will have been achieved to some degree. One must keep in mind that the degree of eigenvalue optimization can be reduced as a sacrifice to the other criteria to be satisfied. Next, special conditions at $M = 0$ and $M = 1$ need to be considered. Among all sparse optimal (or somewhat suboptimal) preconditioners we may select those that have good properties for $M \to 0$, as formulated in criteria 6 (accuracy), 8 (flow-angle insensitivity), 9 (non-parallel eigenvectors), and 10 (minimal vorticity). When extending such preconditioners to higher

TABLE I
Comparison of Preconditioners

	Van Leer	Turkel	Stagnation	Block–Jacobi
Removes stiffness caused by spread in wave speeds	Yes	Yes	Yes	No
Concentrates high-frequency eigenvalues	Yes	Yes	Yes	Yes
Preserves accuracy in incompressilbe limit	Yes	Yes	Yes	No
Decouples acoustic from advective equations	Yes	Not perfectly	Not prefectly	No
Eigenvectors well-behaved in a stagnation point	No	No	Yes	Yes

Mach numbers, we must try to observe conditions 6 (numerical eigenvalue clustering), 11 (continuity at $M = 1$), and, again, 9 (non-parallel eigenvectors).

For construction of new preconditioners by the previous criteria, we start with exploring preconditioning matrices for the 1D Euler equations. Many of the relevant properties of 2D and 3D preconditioners are already found in their 1D counterpart, while application of the design criteria is greatly simplified. This produces some guiding principles for selecting 2D and, ultimately, 3D preconditioners. We also extend the 1D preconditioners to 2D, optimizing design criteria to some extent, excluding some design criteria such as minimization of artificial vorticity production.

6.1. *One-Dimensional Preconditioning Family*

For the one-dimensional Euler equations,

$$\frac{\partial \mathbf{U}}{\partial t} = -\mathbf{A}(\mathbf{U})\frac{\partial \mathbf{U}}{\partial x} = \mathbf{Res}(\mathbf{U}), \tag{27}$$

perfect preconditioning is possible, i.e., the characteristic condition number can be brought down to unity. This is achieved, for instance, by multiplying the residual with the matrix[2]

$$\mathbf{P}_J = q|\mathbf{A}|^{-1}, \tag{28}$$

where q is the flow speed. With the system of symmetrizing variables (2) the detailed matrix becomes

$$\mathbf{P}_J = \begin{pmatrix} \frac{M(M+1+|M-1|)}{2|M^2-1|} & -\frac{M(M+1-|M-1|)}{2|M^2-1|} & 0 \\ -\frac{M(M+1-|M-1|)}{2|M^2-1|} & \frac{M(M+1+|M-1|)}{2|M^2-1|} & 0 \\ 0 & 0 & 1 \end{pmatrix}, \tag{29}$$

[2] This matrix is essentially the diagonal block arising in a Newton solver based on the first-order upwind spatial Euler discretization. This is the only block remaining in point/Jacobi relaxation, therefore, I shall refer to the use of (28) as Jacobi preconditioning.

or

$$\mathbf{P}_{J-sub} = \begin{pmatrix} \frac{M}{1-M^2} & -\frac{M^2}{1-M^2} & 0 \\ -\frac{M^2}{1-M^2} & \frac{M}{1-M^2} & 0 \\ 0 & 0 & 1 \end{pmatrix}, \qquad M < 1; \tag{30}$$

$$\mathbf{P}_{J-super} = \mathbf{P}_{super} = \begin{pmatrix} \frac{M^2}{M^2-1} & -\frac{M}{M^2-1} & 0 \\ -\frac{M}{M^2-1} & \frac{M^2}{M^2-1} & 0 \\ 0 & 0 & 1 \end{pmatrix}, \qquad M > 1. \tag{31}$$

This yields the preconditioned system of equations

$$\frac{\partial \mathbf{U}}{\partial t} = -q|\mathbf{A}|^{-1}\mathbf{A}\frac{\partial \mathbf{U}}{\partial x}; \tag{32}$$

its characteristic speeds are the eigenvalues of $q|\mathbf{A}|^{-1}\mathbf{A}$ and all equal the flow speed in absolute value. This preconditioning is unique for supersonic flow;[3] for subsonic flow there is substantial freedom in choosing a matrix that will achieve perfect preconditioning in the sense of eigenvalue optimization [14]. From (29), (30), (31) it is seen that $\mathbf{P}_J$ is not defined for $M = 1$. It appears that in the preconditioned pressure and velocity equations the residual is artificially blown up by a factor $1/|1 - M^2|$, in order to compensate for the vanishing characteristic speed $u - a_s$. With regard to a numerical update we might interpret this as using a time step for these equations that is inversely proportional to $|1 - M^2|$. In practice this time step must be limited in order to avoid nonlinear instabilities. Note that, when the factor $1/|1 - M^2|$ is taken out, the preconditioner is continuous at $M = 1$. Note further that the entropy equation does not receive this large time step. The use of different Δt for different waves, possible through matrix preconditioning, has been called "characteristic time-stepping" [31], in contrast to just "local time-stepping."

If we allow asymmetry for an arbitrary subsonic optimal preconditioner we can find a two-parameter family of matrices producing optimal eigenvalues,

$$\mathbf{P} = \begin{pmatrix} a & c & 0 \\ d & b & 0 \\ 0 & 0 & 1 \end{pmatrix}. \tag{33}$$

When doing the eigenvalue optimization it turns out that only the product cd, not c or d separately, appears in the constraints on the eigenvalues. This means that the transpose of any optimal preconditioner of the form (33) is also optimal. This, by the way, is not just true for one-dimensional asymmetric preconditioners but holds for any number of dimensions. The proof is trivial; it follows after taking the transpose of the matrix whose eigenvalues are sought.

[3] In the supersonic case, **PA** has three identical eigenvalues($=q$), and for the orthogonal eigenvector structure it must be a multiple of the identity matrix. Hence $\mathbf{P} = q\mathbf{A}^{-1} = q|\mathbf{A}|^{-1}$. In earlier studies, we found the Jordan block form can also keep the same eigenvalues of the system with more degrees of freedom. However, a unique and simple form of the matrix can be obtained even for the additional requirement, orthogonality of the system. Therefore, in order to avoid confusion and unnecessary analysis in obtaining the optimal supersonic preconditioner, we decide to call the supersonic matrix unique.

We shall now try to satisfy the design criteria of Section 4 with the general form (33), suppressing the entropy entry. Most design criteria are relevant even in 1D, except those regarding the vorticity and flow angle, while clustering of numerical eigenvalues becomes trivial in 1D. Decoupling is also trivial, but, at the same time, has an interesting twist; this will be explained at the end of this section.

Satisfying only accuracy, continuity, and optimization of eigenvalues among design criteria, we can propose two families of preconditioners:

$$\mathbf{P}_c = \begin{pmatrix} \frac{M^2}{1-M^2} & \frac{M}{1-M^2}\zeta \\ -\frac{M}{1-M^2} & 1-\frac{\zeta}{1-M^2} \end{pmatrix} \tag{34}$$

and

$$\mathbf{P}_d = \begin{pmatrix} \frac{M^2}{1-M^2} & -\frac{M}{1-M^2} \\ \frac{M}{1-M^2}\delta & 1-\frac{\delta}{1-M^2} \end{pmatrix}. \tag{35}$$

This c– family of preconditioners can be divided into a 1D version of popular multidimensional preconditioners such as symmetric Van Leer–Lee–Roe ($\zeta = -1$), triangular Turkel ($\zeta = 0$), and antisymmetric stagnation preconditioners ($\zeta = 1$). The symmetric Van Leer–Lee–Roe preconditioner produces eigenvectors which become parallel as the Mach number approaches zero, but a 45° angle is maintained as the Mach number approaches one. Next, Turkel's preconditioner causes the eigenvectors to degenerate for both $M = 0$ and $M = 1$. Finally, in D. Lee's stagnation preconditioner, the eigenvectors do not degenerate as M approaches zero,

$$\mathbf{P}_{c,st} = \begin{pmatrix} \frac{M^2}{1-M^2} & \frac{M}{1-M^2} \\ -\frac{M}{1-M^2} & -\frac{M^2}{1-M^2} \end{pmatrix}, \qquad \mathbf{R}_{c,st} = \begin{pmatrix} 1 & -M \\ -M & 1 \end{pmatrix}. \tag{36}$$

For $M \uparrow 1$, however, the eigenvectors of $\mathbf{P}_{c,st}\mathbf{A}$ become parallel; also, $\mathbf{P}_{c,st}$ does not connect smoothly to $\mathbf{P}_{super}$ at $M = 1$. For the moment we shall simply label this member of the c-family as "stagnation preconditioner," although Lee's stagnation preconditioner, as defined in Subsection 5.3, has a more complicated dependence on M.

Interestingly enough, the transpose of these preconditioners, i.e., the d– family, not only produces simpler preconditioned equations, as seen in (37), but also a better eigenvector structure. In particular, the transpose of the stagnation preconditioner, with $\delta = 1$, yields a *diagonal* matrix $\mathbf{P}_{d,st}\mathbf{A}$, with perfectly orthogonal eigenvectors at any Mach numbers:

$$\mathbf{P}_{d,st}\mathbf{A} = a_s \begin{pmatrix} -M & 0 \\ 0 & M \end{pmatrix}, \qquad \mathbf{R}_{d,st} = \begin{pmatrix} 0 & 1 \\ 1 & 0 \end{pmatrix}. \tag{37}$$

The transpose of Turkel's preconditioner has the eigenvector structure

$$\mathbf{R}_{d,T} = \begin{pmatrix} 0 & -2M \\ 1 & 1 \end{pmatrix}, \tag{38}$$

which still degenerates as $M \downarrow 0$, but not as $M \uparrow 1$.

Among the above c– and d– families of preconditioners, a preconditioner with proper ζ and δ functions can be formulated in order to satisfy all 1D design criteria. This new preconditioner will be evaluated with regard to each design condition.

(1) *Accuracy and continuity.* The artificial viscosity analysis of Turkel *et al.* [30] shows that element a must be $\mathcal{O}(M^2)$ to preserve the accuracy for very low Mach numbers. Note that this condition is not met in the preconditioner $\mathbf{P}_{J-sub}$, in Eq. (30), since its element a for subsonic flow equals $M/(1-M^2)$. However, $c-$ and $d-$ families reduce a down to $M^2/(1-M^2)$, ensuring accuracy preservation in the incompressible limit. These also yield the proper transition at $M=1$ to the unique supersonic value $M^2/(M^2-1)$; see Eq. (31).

(2) *Optimizing eigenvalues.* The optimal eigenvalue restriction requires that the eigenvalues λ_1, λ_2 of $\mathbf{PA}$ must have opposite signs with the same quantity, i.e., $\lambda_{1,2} = \pm M$ for $M < 1$. The above $c-$ and $d-$ families of preconditioners have these optimized eigenvalues.

(3) *Positivity and symmetrizability.* Next we consider positivity of $\mathbf{P}$ and symmetrizability of the preconditioned system.

DEFINITION 1. A matrix M is called positive definite if and only if $x^T Mx > 0$ for all nonzero x; if M is positive definite, so is M^T.

Considering first the $c-$family, with regard to positivity of $\mathbf{P}_c$,

$$\vec{x} \cdot \mathbf{P}_c \vec{x} = \frac{1}{1-M^2}\left[\left(M^2 x_1^2 + \frac{\zeta-1}{2}x_2\right)^2 + \left\{1 - M^2 - \left(\frac{\zeta+1}{2}\right)^2\right\}x_2^2\right]; \quad (39)$$

this is positive for $\vec{x} \neq \vec{0}$ if

$$-1 - 2\sqrt{1-M^2} < \zeta < -1 + 2\sqrt{1-M^2}. \quad (40)$$

Figure 7 shows that the positivity can be preserved only if the preconditioner remains inside of this elliptic domain. The stagnation preconditioner and its transpose matrix fail to preserve the positivity for all $M < 1$, while Turkel's are non-positive for $M \geq \sqrt{3}/2$; only $\mathbf{P}_{\text{VLR}}$ is positive-definite at all $M < 1$.

DEFINITION 2. If the equations can be put into the form

$$\mathbf{Q}\partial_t \mathbf{v} + \mathbf{A}^* \partial_x \mathbf{v} + \mathbf{B}^* \partial_y \mathbf{v} + \mathbf{C}^* \partial_z \mathbf{v} = 0, \quad (41)$$

where $\mathbf{Q}$, $\mathbf{A}^*$, $\mathbf{B}^*$, $\mathbf{C}^*$ are all symmetric, and $\mathbf{Q}$ is positive definite, then the system is called symmetrizable, and it can be shown that the solution is stable in the norm $(\mathbf{v^T Q v})$.

The limits of the symmetrizability interval are always positive, except one choice of $\zeta(M)$:

$$\zeta(M) = -M^2. \quad (42)$$

For this choice of $\zeta(M)$ the symmetrizability is lost by a non-positive definite $\mathbf{Q}$.

(4) *Orthogonalizing eigenvectors.* As has been shown already, the stagnation preconditioner has orthogonal eigenvector structure when Mach number approaches zero and the Van Leer–Lee–Roe preconditioner has an orthogonal system at sonic point; the small circles in Fig. 7 indicate the points of orthogonalizing ζ values. To orthogonalize eigenvectors for all Mach numbers, the inner product of preconditioned Jacobian eigenvectors needs to

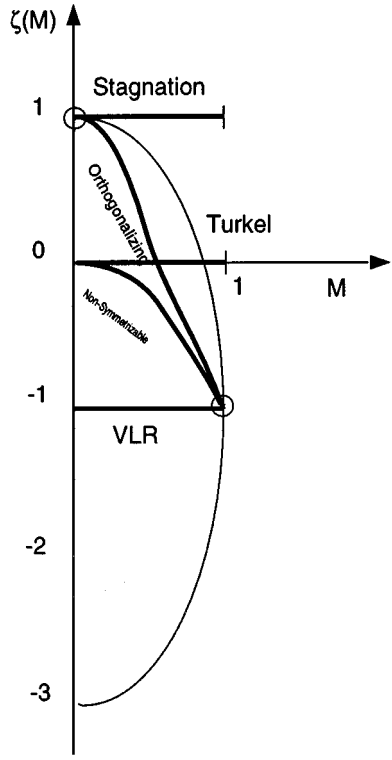

FIG. 7. Members of the *c*–family of preconditioners. Positivity is preserved only inside of this elliptic domain.

vanish.[4] This can be achieved for all M by taking

$$\zeta = 1 - \frac{4M^2}{1+M^2}. \tag{43}$$

This function connects the above orthogonalizing limit points through the positivity domain. Figure 7 shows the graph of the $\zeta(M)$ function in the positivity domain, and some other choices of ζ, including the form (43) which orthogonalizes the eigenvectors of **PA**. The graph of the latter is tangent to the graph of (42), so the orthogonality choice preserves symmetrizability.

The *d*–family, attractive because of its algebraic simplicity, does not have such an outstanding member. There is one choice for which the orthogonal eigenvector structure is preserved, namely, $\delta(M) = 1$ (transpose of the stagnation preconditioner), but this matrix is not positive definite and does not connect smoothly to the supersonic branch (see Fig. 8).

The characteristic equations for the resulting *c*–family preconditioned system can be written as

$$\mathbf{V}_t^{(1)} + u\mathbf{V}_x^{(1)} = 0 \tag{44}$$

$$\mathbf{V}_t^{(2)} - u\mathbf{V}_x^{(2)} = 0, \tag{45}$$

[4] The alternate method is to force the resulting matrix to be symmetric (i.e., $\mathbf{PA} = (\mathbf{PA})^{\mathbf{T}}$).

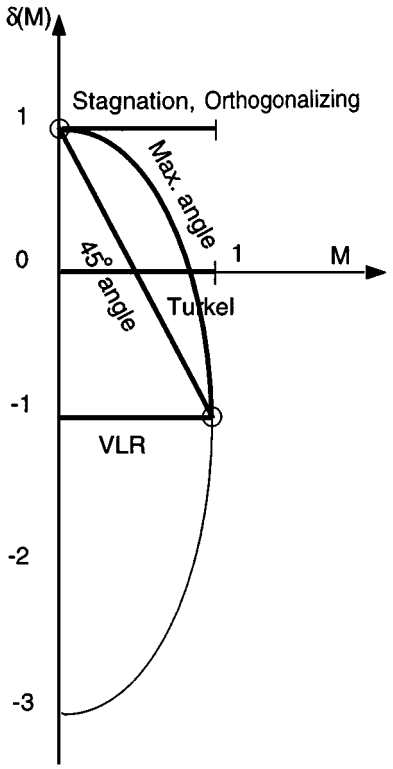

FIG. 8. Members of the d–family of preconditioners. Positivity is preserved only inside of this elliptic domain.

where

$$\partial \mathbf{V}^{(1)} = \frac{\partial p}{\rho} + u\partial u \tag{46}$$

$$\partial \mathbf{V}^{(2)} = (1 - 2M^2 - \zeta)\frac{\partial p}{\rho} + u(\zeta + 1)\partial u. \tag{47}$$

The first characteristic equation of the forward moving wave describes convection of total enthalpy in isentropic flow. As seen from the equation, ζ is dropped out, indicating that the total enthaply is still preserved even after preconditioning. However, this total enthaply convection is not valid for the $d-$ family of the preconditioner. It is also seen that the invariant value 1 in element (2, 2) of the optimal preconditioner becomes the scale factor of the enthalpy-wave speed, and this remains true in 2D and 3D. In 1D the enthalpy wave replaces the forward acoustic wave of the original system; in 2D and 3D, however, it replaces a shear wave or, more precisely, the convection of the normal component of velocity.

The following analysis shows how the preconditioned equations are affected by the eigenvector angle. In the case of parallel eigenvectors, the same flow quantity (Riemann invariant) has to propagate at two different characteristic speeds, which produces the ill-conditioned unstable system. In contrast, with an orthogonal eigenvector structure independent quantities propagate with different velocity. This is illustrated below in a few examples.

By taking $\zeta = -1$ (VLR), the second invariant $\partial \mathbf{V}^{(2)} = \frac{\partial p}{\rho}$ approaches the other invariant (enthalpy) for $M \downarrow 0$, but it remains distinct (although not completely independent) as $M \uparrow 1$.

For $\zeta = 0$ (Turkel) it approaches the other invariant for $M = 0$ as well as $M = 1$. For $\zeta = 1$ (D. Lee, stagnation), it approaches the other for $M = 1$, but for $M = 0$ it becomes completely independent.

For $\zeta = 1 - \frac{4M^2}{1+M^2}$, the top choice, we find

$$\partial \mathbf{V}^{(2)} = M \frac{\partial p}{\rho} - a_s \partial u, \tag{48}$$

which again remains distinct from $\partial \mathbf{V}^{(1)}$ for any M; in the $(\frac{\partial p}{\rho}, \partial u)$ plane, these two invariants form orthogonal vectors. This choice produces a well-balanced preconditioned system,

$$\left(\frac{p_t}{\rho a_s} + M u_t \right) + u \left(\frac{p_x}{\rho a_s} + M u_x \right) = 0; \tag{49}$$

$$\left(M \frac{p_t}{\rho a_s} - u_t \right) - u \left(M \frac{p_x}{\rho a_s} - u_x \right) = 0. \tag{50}$$

It resembles the original characteristic equations, preserving its orthogonal character with the benefit of equal absolute characteristic speeds. At $M = 1$ the characteristic variables become equal to the original Riemann invariants; this remains so for $M > 1$ when using $\mathbf{P}_{super} = q\mathbf{A}^{-1}$. This is as close to the original physics as one can ever get after preconditioning.

6.2. *Two-Dimensional Preconditioner Family*

When charting the huge family of 2D Euler preconditioners, our thorough knowledge of the 1D family offers very helpful guidance. It turns out that the useful part of the 2D family is not so large, after all, with only one obvious extra parameter, and satisfying all the criteria of Section 4 becomes impossible. Waves may now propagate in any direction, with speed and the associated eigenvector depending on the propagation angle θ; in addition there is a structure of 3 rather than 2 eigenvectors to be kept from degenerating. In this section we shall do an initial search for and evaluation of 2D preconditioners; the further subsections of this section deal with meeting specific design criteria. Particular attention will be given to optimization of eigenvalues for cells with an aspect ratio $\mathcal{AR} \neq 1$, reducing the sensitivity of the preconditioner to the flow angle, especially near a stagnation point (Subsection 5.3), and to preventing eigenvector degeneration in the preconditioned system.

The 2D version of the Van Leer–Lee–Roe preconditioner (11) produces an unsteady version of the characteristic equations of steady supersonic flow [17],

$$\begin{aligned} (\partial_t + \beta a_s \partial_s + a_s \partial_n) \left(\partial p + \frac{\rho q}{\beta} \partial v \right) &= 0, \\ (\partial_t + \beta a_s \partial_s - a_s \partial_n) \left(\partial p - \frac{\rho q}{\beta} \partial v \right) &= 0, \\ H_t + q H_s &= 0, \\ S_t + q S_s &= 0, \end{aligned} \tag{51}$$

where H and S are total enthalpy and entropy, respectively.[5]

[5] This matrix is not the only 2D supersonic preconditioner that can produce the ideal condition number $K = 1$.

In addition to enthalpy and entropy convected in the flow direction at the flow speed q, the two steady-flow Riemann invariants are convected along the Mach lines,[6] also at the flow speed. Thus, the condition number equals 1 for all $M > 1$.

Using the sparseness pattern of $\mathbf{P}_{super}$, we restrict our research for subsonic preconditioners to matrices of the form

$$\mathbf{P}_{sub} = \begin{pmatrix} a & c & 0 & 0 \\ d & b & 0 & 0 \\ 0 & 0 & e & 0 \\ 0 & 0 & 0 & 1 \end{pmatrix}, \tag{52}$$

with only one additional parameter e, compared to the 1D case. Since the entropy equation is unaffected, we shall drop the entropy entries in what follows.

In comparison to the 1D case there is a fundamental difference. In 1D the forward acoustic wave becomes the enthalpy wave; in 2D the enthalpy wave is still present, but in each propagation direction a distinct forward quasi-acoustic wave can be identified: its speed is ruled by the value of element e.

(1) *Optimizing eigenvalues and accuracy.* By the study of wave propagation analysis, we can propose a one-parameter family of matrices which produce optimal wave patterns [13]; with $c = M\zeta(M)/\sqrt{1-M^2}$ it takes the form

$$\mathbf{P} = \begin{pmatrix} \frac{M^2}{\beta} & \frac{M}{\beta}\zeta & 0 \\ -\frac{M}{\beta} & 1-\frac{\zeta}{\beta} & 0 \\ 0 & 0 & \beta \end{pmatrix}, \tag{53}$$

where $\beta = \sqrt{1-M^2}$ for subsonic flow. Again, the Van Leer–Lee–Roe and Turkel matrices are obtained for $\zeta = -1$ and 0, respectively. A variant of the 2D stagnation preconditioner, which will be derived in the next section, can be obtained by setting $\zeta = 1$. Accuracy preservation for the low Mach number can be met by setting element a $\mathcal{O}(M^2)$.

(2) *Positivity.* Positivity of $\mathbf{P}$ for the above choice of $\zeta(M)$ is easily established. The positivity analysis for the 2D ζ–family is very similar to the 1D analysis in Subsection 6.1. The essential change is that the denominator $1-M^2$ or β^2, found in the elements of $\mathbf{P}$, is replaced by $\sqrt{1-M^2}$, or β. The third component, x_3, of the test vector $\vec{x}$ arising in the 2D analysis, does not affect positivity for their family of preconditioners. Therefore, for positivity we require

$$-1 - 2\sqrt{\beta} < \zeta < -1 + 2\sqrt{\beta}. \tag{54}$$

When comparing this to the 1D variant, Eq. (40), we see that, owing to the replacement of β by $\sqrt{\beta}$, the allowed range for $\zeta(M)$ is a little wider in the 2D case. The conclusions about the positivity of the various known preconditioners are not changed: $\zeta = 1$ violates positivity for all M, $\zeta = 0$ violates positivity for the larger values of M (in this case, for $M \geq \frac{\sqrt{15}}{4}$), and $\zeta = -1$ and the function (56) both lie in the positivity range for all M.

[6] The Mach lines are steady wave patterns at angles $\pm\mu$, where $\mu = \arcsin(1/M) = \arctan(1/\sqrt{M^2-1})$ is the Mach angle.

(3) *Orthogonalizing eigenvectors.* For orthogonalizing preconditioned systems, we need to study the eigenvectors of matrix coefficients along and normal to the streamwise directions. The right eigenvectors associated with enthalpy and two acoustic waves ($\lambda_1 = q$, $\lambda_{2,3} = \pm q\beta$ for **PA** and $\lambda_1 = 0$, $\lambda_{2,3} = \pm q$ for **PB**), respectively, are

$$\mathbf{R_{PA}} = \begin{pmatrix} M(1+\zeta) & 0 & -M \\ \beta - M^2 - \zeta & 0 & 1 \\ 0 & 1 & 0 \end{pmatrix}, \qquad \mathbf{R_{PB}} = \begin{pmatrix} 0 & M & -M \\ 1 & -1 & 1 \\ 0 & \beta & \beta \end{pmatrix}. \tag{55}$$

As can be seen from the previous eigenvector system, **PB** does not have any dependence on the variation of ζ and two acoustic eigenvectors become parallel as the Mach number approaches 1. However, this parallelity of eigenvectors at the sonic point is not much of a problem because numerical practice shows the numerical instabilities with the use of preconditioning usually occurs around the stagnation point. At a stagnation point, **PB** maintains 45° between eigenvectors, which is an acceptable eigenvector structure. The system still degenerates as a whole since no eigenvector spans the first row, but it is confined to only normal to the flow direction ($\theta = 0$). However, it appears to be enough to establish eigenvector orthogonality only when $\theta = 0$, i.e., **PA**, for all Mach numbers.

Orthogonality of the first and third eigenvectors of **PA** occurs for a value of $\zeta(M)$ different from (43), because of the appearance of $\sqrt{1-M^2}$ instead of $1 - M^2$. The orthogonalizing choice becomes

$$\zeta(M) = \frac{\beta - 2M^2}{1 + M^2}. \tag{56}$$

This new preconditioner produces perfectly orthogonal eigenvectors for waves moving in the streamwise direction for all Mach numbers, as well as satisfaction of symmetrizability and positivity conditions. In spite of the complicated form of (56), the numerical implementation of this matrix is quite simple because any matrix of the form (53) produces simply structured artificial-viscosity matrices, which does not depend on the specific choice of ζ. It is noted that the construction of artificial-viscosity matrices becomes complicated by the method of limiting the value of M in the preconditioner to prevent parallel eigenvectors, suggested by Darmofal and Schmid [4].

The above analysis gives priority to a certain choice of design criteria, which, to some extent, is a matter of taste, and clearly could vary with the intended application. When other sets of criteria are emphasized, different matrices will result, since no matrix can satisfy all criteria.

7. NUMERICAL STUDIES

For the validation of the stagnation preconditioner and comparsion on performance of other Van Leer and Turkel preconditioners and those variants, three numerical tests were performed. In those cases, the stagnation preconditioner improved stability as well as convergence in stagnation regions.

The first numerical test is the calculation of the evolution of a one-point flow-angle disturbance in a square domain, as in Subsection 5.2. (This model problem tests how well flow-angle differences between the cells can be damped out. Figure 4 shows the initial

TABLE II
Maximum Bearable Initial Perturbation Angle

CFL	Un PC	Van Leer	Van Leer-sub	Turkel	Stagnation
0.5	180	129	137	149	161
0.7	180	61	133	149	155
0.8	180	50	94	149	117

Note. CFL = CFL number; Un PC = no preconditioning; Van Leer = Van Leer–Lee–Roe preconditioner; Van Leer-sub = suboptimal variant of Van Leer–Lee–Roe preconditioner; Turkel = Turkel preconditioner; Stagnation = stagnation preconditioner with the principal angle of local flow angle; $M = 0.1$, 10×10 grid.

conditions and the resulting converged (uniform) solution. Table II shows the maximum perturbation angles allowed by each of the preconditioners as a function of the CFL number used. In case the streamwise stagnation preconditioner is used, the angle sensitivity appears to be reduced in comparison with the Van Leer preconditioner and also (for the smaller CFL numbers) the Turkel preconditioner.

The second test is the calculation of stagnation flow. As shown earlier in Fig. 5, the Van Leer–Lee–Roe preconditioner (without "fix") is not able to calculate stagnation flow and neither is Turkel's preconditioner. Note that the original form of Turkel's preconditioner is tested, meaning it does not contain a low Mach number cutoff on its element. However, as shown by Fig. 9, the stagnation preconditioner is able to compute this flow successfully in the half-plane domain. If the stagnation preconditioner is used with $b_0 = 0$ in a full-plane calculation, it produces a large amount of artificial vorticity near the stagnation point. In consequence, the velocity vectors at the stagnation point are rotated counterclockwise, eventually leading to slow divergence.

The preconditioned vorticity equation shows that there is too much vorticity production by the combined velocity and pressure fields, and that the vorticity-convection term is not

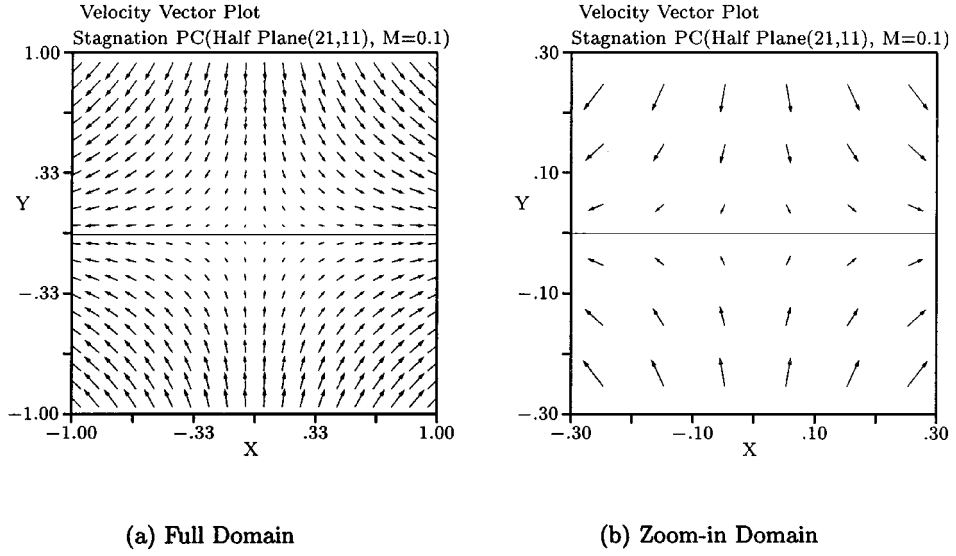

(a) Full Domain (b) Zoom-in Domain

FIG. 9. Flow field of half-plane stagnation flow, computed with the "streamwise stagnation preconditioner." The upper plane is for $b_0 = 0$; the lower plane for $b_0 = 1.5$.

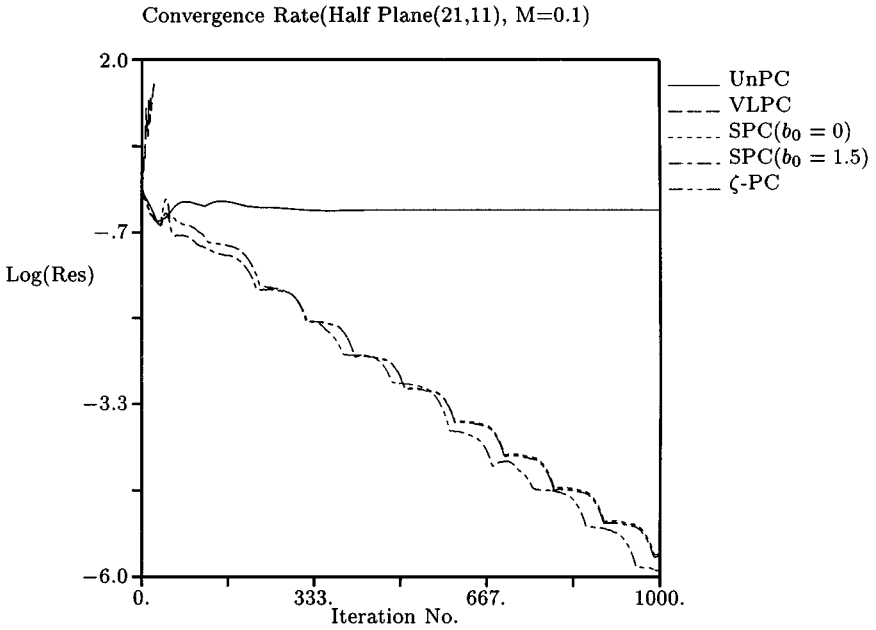

FIG. 10. Residual history for half-plane stagnation flow calculation. UnPC = unpreconditioned; SPC = stagnation preconditioning; VLPC = Van Leer–Lee–Roe preconditioner (divergent calculation). Note: the Turkel preconditioner also fails to converge in this test.

well defined, as it is in the unpreconditioned and symmetrically preconditioned cases. The analysis shows that b_0 needs to be $2/M^2$ in order to maintain a well-defined vorticity-convection term. However, choosing $b_0 > 2/M^2$ causes the loss of positivity and symmetrizability, and actually makes the system lose hyperbolicity. Instead, simply increasing b_0 to 1.5 reduces the vorticity production substantially.

In order to reduce the extent of vorticity production, the stagnation-flow calculations were performed in the half-plane, with an imaginary-wall boundary (flow symmetry) condition. With this set-up, the streamwise stagnation preconditioner succeeds in removing the stagnation instability and speeding up the convergence without any problem. Figure 9 shows that the final converged solution does not have so much vorticity production, and Fig. 10 demonstrates the convergence acceleration. It is seen that the stagnation preconditioner greatly improves the convergence speed, while the Van Leer–Lee–Roe and Turkel preconditioner blows-up due to the stagnation instability, and the unpreconditioned case stalls due to the low Mach-number stiffness. It was observed that the increase of b_0 to 1.5 gives slightly faster convergence than with $b_0 = 0$ since this reduces the vorticity production and, in addition, ensures the positive-definiteness and symmetrizability of the system. The same two numerical tests with the new stagnation-friendly all-purpose ζ-preconditioner (53), (56) shows that it is also robust with accelerated convergence slightly faster than the stagnation preconditioner.

As another more practical numerical test, the Van Leer, Turkel, and stagnation preconditioners were used in computing steady two-dimensional flows about a NACA 0012 airfoil, showing how these behave in the low Mach-number limit. The computations were made with first-order upwind differencing on two *O*-grids, with 31×16 and 61×31 cells; the grids are too coarse for good accuracy, but this brings out the differences in quality between

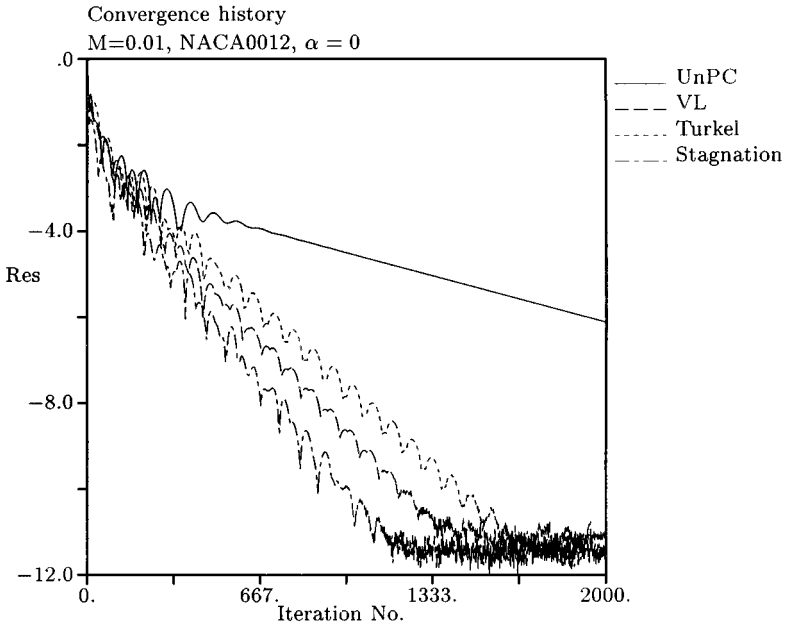

FIG. 11. Residual history for low-speed flow around NACA 0012 airfoil; $M = 0.01$, 31×16 grid; pressure-extrapolation wall-boundary procedure; UnPC = Unpreconditioned; VL = Van Leer preconditioner; Turkel = Turkel preconditioner; Stagnation = stagnation preconditioner. The ζ– preconditioner produces the same convergence history as the stagnation preconditioner.

the solutions. Furthermore, on coarse grids it is not necessary to use the stagnation-point "fix" of Darmofal and Schmidt [4] for the Van Leer and Turkel matrices. Time-marching was done by a single-stage scheme, so there is no strong high-frequency damping to help the local preconditioning in the accelerating convergence. The CFL number for the local time step was set to 0.5.

Figure 11 shows the residual history on the 31×16 grid for low-speed flow, $M_\infty = 0.01$, $\alpha = 0^\circ$. It is seen that all these preconditioners successfully accelerate the convergence compared to the non-preconditioned scheme, with the stagnation preconditioner performing best, and Turkel's worst. Observe, however, the oscillatory residual convergence when preconditioning is used. These oscillations are found to be generated at the leading and trailing edges, and most likely are due to vorticity generation during wave reflections.

Figures 12–15 show several converged solutions obtained without and with preconditioning. The pressure boundary condition is used for better numerical solution at a wall boundary. As was discussed in Section 3, the unpreconditioned upwind scheme does not preserve the accuracy in the low-speed limit. Figure 12 illustrates that, as the Mach number goes down to 0, the solution quality gets more degraded. In contrast, calculation with the Van Leer–Lee–Roe and stagnation preconditioners produces reasonably accurate solutions even at $M = 0.01$, as can be seen in Figs. 13 and 15.

However, all those preconditioners without a low Mach-number cutoff on its element fail to speed up the convergence with a more finer grid such as 121×61. This indicates that the stagnation preconditioner and ζ– preconditioner may improve stability to some extent, but those modifications and new development of a preconditioner on the matrix structure level are still not enough to overcome completely so many instability causes in Subsection 5.1.

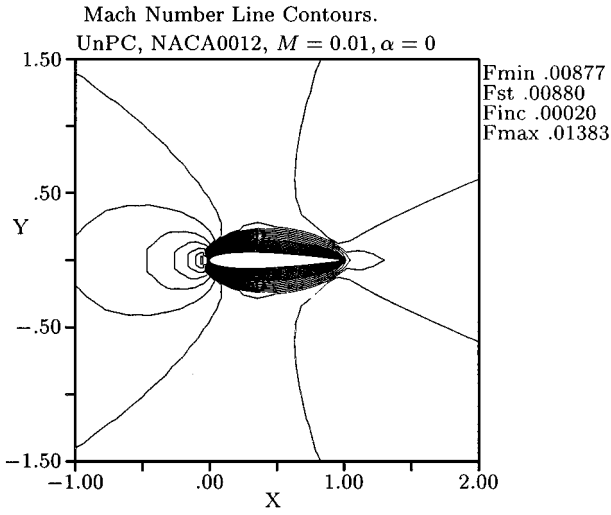

FIG. 12. Mach number contours for unpreconditioned steady solution with the pressure-extrapolation boundary condition; NACA 0012, $M = 0.01$, 31×16 grid.

8. CONCLUSIONS

The traditional goal for the Euler preconditioning has been to produce optimal wave fronts with the lowest possible condition number, because this minimization of the characteristic-speed spread has a beneficial effect on the convergence acceleration. Further research has shown that, in addition to the basic advantage of stiffness removal, the preconditioning can produce other major benefits such as system behavior like a scalar equation, accuracy preservation in the incompressible limit, and decoupling of the Euler equations into elliptic

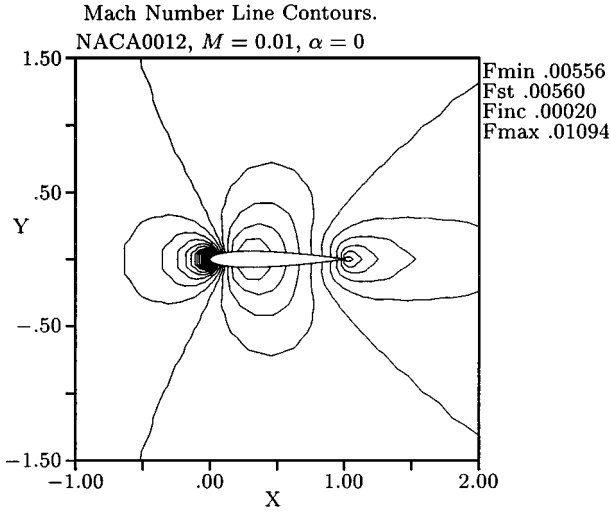

FIG. 13. Mach number contours for preconditioned steady solution with the pressure-extrapolation boundary-condition; NACA 0012, $M = 0.01$, 31×16 grid; Van Leer preconditioner. The same solution is obtained with the stagnation and $\zeta-$ preconditioner.

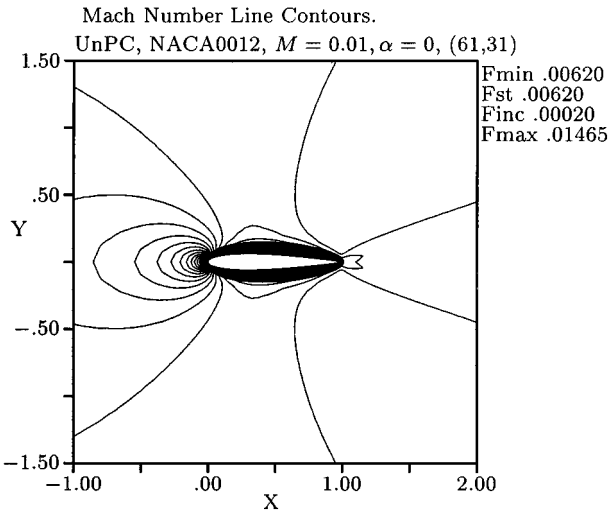

FIG. 14. Mach number contours for unpreconditioned steady solution with pressure-extrapolation boundary-condition; NACA 0012, $M = 0.01$, 61×31 grid.

and hyperbolic parts. However, in spite of these benefits, the use of preconditioning until now has been severely restricted, mainly because of the instability arising near a stagnation point. Analyzing the above benefits and problems in detail yields a list of design criteria for preconditioners: positivity, symmetrizability of the preconditioned system, reduction of eigenvalue spread, decoupling within the system, sparseness, clustering of numerical eigenvalues, accuracy preservation in the incompressible limit, flow-angle insensitivity, non-parallelism of eigenvectors, minimum vorticity production, and continuity at a sonic point. We have discussed cause and effect at some length with regard to all these design criteria.

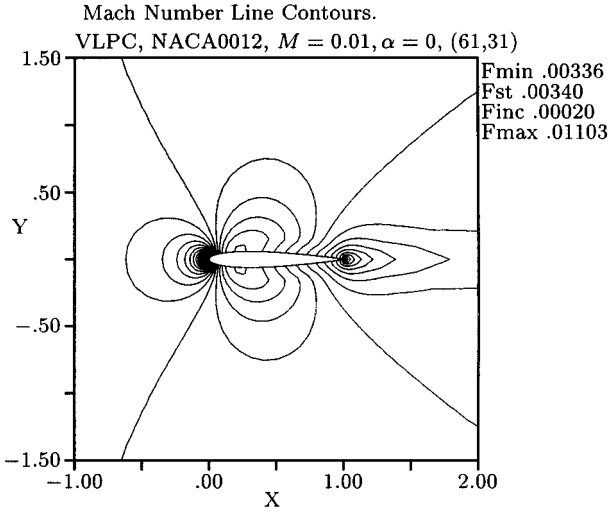

FIG. 15. Mach number contours for preconditioned steady solution with pressure-extrapolation boundary-condition; NACA 0012, $M = 0.01$, 61×31 grid; Van Leer preconditioner. The same solution is obtained with the stagnation and $\zeta-$ preconditioner.

Having clearly defined the above design criteria, it becomes possible to derive families of 1D and 2D preconditioning matrices that meet most design criteria. In particular, the attempt to develop a new preconditioner by constructing an orthogonal eigenvector structure without any "fix" or "limiter" in the entries for low Mach number is a fresh approach, because the manipulation of eigenvectors in addition to eigenvalues has been regarded in a very limited way or considered nearly impossible. This construction of non-parallel eigenvectors was motivated by the success of the "stagnation preconditioner," which was designed in order to reduce the angle dependence in a preconditioner, but later was proven to prevent degeneration of eigenvectors in the low-speed limit.

The robustness problem related to stagnation instability involves a number of detailed issues, such as flow-angle sensitivity of the preconditioner, parallel eigenvectors, and excessive artificial vorticity production. To help cure the instability, special boundary procedures were suggested; more importantly, the newly developed stagnation preconditioner has non-parallel eigenvectors and a weak angle dependence for low Mach numbers, and serves as a model for constructing more robust preconditioned systems.

We have demonstrated that the stagnation preconditioner and a sub-optimal variant of the Van Leer–Lee–Roe preconditioner, the result of another attempt to improve robustness, can sustain a larger flow-angle difference between cells in the flow-angle perturbation test. Furthermore, the stagnation preconditioner is the only one, among preconditioners tested, that can converge to the steady solution of the low-speed stagnating-flow test problem. Some calculations of inviscid flow around airfoils on coarse grids are presented, showing, among other things, that the stagnation and Van Leer preconditioners are comparable in their ability to accelerate convergence and preserve accuracy in the incompressible limit.

In some practical tests with much finer grids, the stagnation and $\zeta-$ preconditioners, without the use of a cutoff for the preconditioner element, still fall short in producing completely stable solutions. This implies that the stagnation and $\zeta-$ preconditioners need a combination of other numerical techniques such as cutoff and modification of the artificial-viscosity treatment for more practical usage. However, more importantly, these new preconditioners provide much improvement with regard to many design criteria, as has been shown by analysis as well as some numerical tests.

APPENDIX 1: EQUATION FOR THE WAVE-FRONT ENVELOPE

In Fig. 16, L_1 and L_2 are two wave-front lines coresponding to wave-speeds λ_1 and λ_2 and wave-angles θ_1 and θ_2.

Their intersection point (X, Y) can be obtained by solving the two equations

$$\frac{Y-\lambda_1 \sin\theta_1}{X-\lambda_1 \cos\theta_1} = -\frac{1}{\tan\theta_1}, \tag{57}$$

$$\frac{Y-\lambda_2 \sin\theta_2}{X-\lambda_2 \cos\theta_2} = -\frac{1}{\tan\theta_2}, \tag{58}$$

where Eq. (57) represents the points of line L_1 and Eq. (58) represents the points of line L_2.

To solve for the wave-front envelope, first let L_2 approach L_1; this means

$$\begin{aligned} \lambda_2 &= \lambda_1 + \lambda_1{}'\Delta\theta, \\ \theta_2 &= \theta_1 + \Delta\theta. \end{aligned} \tag{59}$$

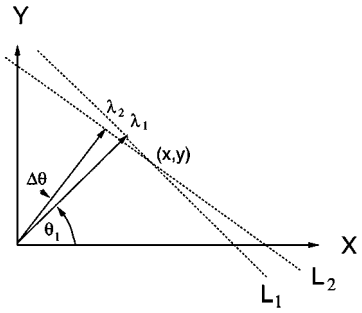

FIG. 16. Two intersecting wave-front lines.

Substituting for λ_2 from Eq. (59) in Eq. (58), and solving simultaneously with Eq. (57) for (X, Y), we obtain, for $\Delta\theta \to 0$,

$$X = \lambda_1 \cos\theta_1 - \lambda_1' \sin\theta_1,$$
$$Y = \lambda_1 \sin\theta_1 + \lambda_1' \cos\theta_1.$$

Second, replace λ_1 and θ_1 by $\lambda(\theta)$ and θ so as to represent all possible wave-angles in the envelope; in vector/matrix notation this gives

$$\begin{pmatrix} X \\ Y \end{pmatrix} = \begin{bmatrix} \cos\theta & -\sin\theta \\ \sin\theta & \cos\theta \end{bmatrix} \begin{pmatrix} \lambda(\theta) \\ \lambda'(\theta) \end{pmatrix}. \tag{60}$$

This is the equation for the wave-front envelope.

APPENDIX 2: VARIOUS EULER PRECONDITIONERS AND ARTIFICIAL VISCOSITY MATRICES

The Van Leer–Lee–Roe preconditioner is

$$\mathbf{P}_{\mathrm{VLR}} = \begin{pmatrix} \frac{\tau}{\beta^2}M^2 & -\frac{\tau}{\beta^2}M & 0 & 0 \\ -\frac{\tau}{\beta^2}M & \frac{\tau}{\beta^2}+1 & 0 & 0 \\ 0 & 0 & \tau & 0 \\ 0 & 0 & 0 & 1 \end{pmatrix},$$
$$\mathbf{P}_{\mathrm{VLR-subotpimal}} = \begin{pmatrix} \alpha\frac{M^2}{\beta} & -\alpha\frac{M}{\beta} & 0 & 0 \\ -\alpha\frac{M}{\beta} & \alpha\left(\frac{1}{\beta}+1\right) & 0 & 0 \\ 0 & 0 & \beta & 0 \\ 0 & 0 & 0 & \alpha \end{pmatrix}, \tag{61}$$

where $\beta = \sqrt{|1-M^2|}$, $\tau = \beta$ (β/M for supersonic), and $\alpha = \frac{1}{2}$ for low M and 1 for high M. The sub-optimal version was developed for reducing the flow-angle sensitivity.

The Turkel preconditioner is

$$\mathbf{P}_{\mathrm{T}} = \begin{pmatrix} \frac{M^2}{\beta} & 0 & 0 & 0 \\ -\frac{M}{\beta} & 1 & 0 & 0 \\ 0 & 0 & \beta & 0 \\ 0 & 0 & 0 & 1 \end{pmatrix}, \qquad \mathbf{P}_{\mathrm{T-mod}} = \begin{pmatrix} (1+\epsilon)\frac{M^2}{\beta} & 0 & 0 & 0 \\ -\frac{M}{\beta} & 1 & 0 & 0 \\ 0 & 0 & 1 & 0 \\ 0 & 0 & 0 & 1 \end{pmatrix}, \tag{62}$$

with $\epsilon > 0$ for symmetrizability. In numerical tests, the original Turkel preconditioner is used with setting the (3, 3) element to 1. The transpose of $\mathbf{P}_{\mathrm{T}}$ produces no artificial vorticity.

The stagnation preconditioner is

$$\mathbf{P}_{\mathrm{stag,streamwise}} = \begin{pmatrix} M^2 & M\sqrt{1+M^2} & 0 & 0 \\ -M\sqrt{1+M^2} & (b_0-1)M^2 & 0 & 0 \\ 0 & 0 & 1 & 0 \\ 0 & 0 & 0 & 1 \end{pmatrix}, \tag{63}$$

where $b_0 = 0$ for the optimal wave pattern. The modified version is with $b_0 > 1$ for positive definiteness and symmetrizability.

The $\zeta-$ preconditioner for all purposes is

$$\mathbf{P}_{\zeta} = \begin{pmatrix} \frac{M^2}{\beta} & \zeta\frac{M}{\beta} & 0 & 0 \\ -\frac{M}{\beta} & -\frac{\zeta}{\beta}+1 & 0 & 0 \\ 0 & 0 & \beta & 0 \\ 0 & 0 & 0 & 1 \end{pmatrix}, \tag{64}$$

where $\zeta = -1$ for the Van Leer preconditioner, $\zeta = 0$ for the Turkel preconditioner, and $\zeta = 1$ for an approximation of the stagnation preconditioner with $b_0 = 1.5$ in the incompressible limit.

The preconditioned residual computed by integration over a finite volume (a quadrilateral cell) is expressed conservatively for artificial viscosity,

$$(\tilde{\mathbf{P}}\ \mathbf{Res})_{i,j} = -\frac{1}{V_{i,j}}\mathbf{P}_{i,j}\sum_{k=1}^{4}\{\mathbf{\Phi}_k \Delta S_k\}_{i,j}\,, \tag{65}$$

where $V_{i,j}$ is the area of the cell, ΔS_k is the length of the kth cell face, $\mathbf{\Phi}_k$ is flux normal to the kth cell face, and $\mathbf{P}_{i,j}$ is the preconditioner which is evaluated at cell center.

For the conservative scheme, the modified flux becomes

$$\mathbf{\Phi}^{\mathrm{mod}}_{\mathrm{Euler,upwind}} = \frac{1}{2}(\mathbf{\Phi}_L + \mathbf{\Phi}_R) - \frac{1}{2}|\hat{\mathbf{\Omega}}|^{\mathrm{mod}}(\mathbf{U}_R - \mathbf{U}_L), \tag{66}$$

where the modified artificial-viscosity matrix $|\hat{\mathbf{\Omega}}|^{\mathrm{mod}}$ is defined as

$$|\hat{\mathbf{\Omega}}|^{\mathrm{mod}} = \mathbf{M}\mathbf{Q}\left(\hat{\mathbf{P}}_{2D}^{-1}|\hat{\mathbf{P}}_{2D}\hat{\mathbf{A}}_{\parallel}\cos(\phi_{\parallel}-\theta)| + \hat{\mathbf{P}}_{2D}^{-1}|\hat{\mathbf{P}}_{2D}\hat{\mathbf{A}}_{\perp}\cos(\phi_{\perp}-\theta)|\right)\mathbf{Q}^{-1}\mathbf{M}^{-1}, \tag{67}$$

where $\mathbf{Q}$, $\mathbf{Q}^{-1}$ are transformations between Cartesian coordinates and flow-aligned coordinates, and $\mathbf{M}$, $\mathbf{M}^{-1}$ are transformations between the different set of variables. In order to

avoid a stagnation instability problem, the factors $\mathbf{P}^{-1}$ are needed to (more or less) cancel the preconditioning matrix $\tilde{\mathbf{P}}_{i,j}$ multiplying the full residual.

For symmetrizing variables and stream-aligned coordinates, $\mathbf{P}_{\mathrm{VLR}}$ and $\mathbf{P}_{\mathrm{VLR-subotpimal}}$ produce the artificial-viscosity matrices

$$\hat{\mathbf{P}}_{2D}^{-1}|\hat{\mathbf{P}}_{2D}\hat{\mathbf{A}}_{\parallel}| = \hat{a}_s \begin{pmatrix} \frac{|\hat{M}^2-1|+1}{\hat{M}} & 1 & 0 & 0 \\ 1 & \hat{M} & 0 & 0 \\ 0 & 0 & \hat{M} & 0 \\ 0 & 0 & 0 & \hat{M} \end{pmatrix};$$

$$\hat{\mathbf{P}}_{2D}^{-1}|\hat{\mathbf{P}}_{2D}\hat{\mathbf{A}}_{\perp}| = \hat{a}_s \begin{pmatrix} \frac{\hat{\beta}}{\hat{M}\sqrt{\hat{\alpha}}} & 0 & 0 & 0 \\ 0 & 0 & 0 & 0 \\ 0 & 0 & \frac{\hat{M}\sqrt{\hat{\alpha}}}{\hat{\beta}} & 0 \\ 0 & 0 & 0 & 0 \end{pmatrix}. \tag{68}$$

With the original Turkel preconditioner (assuming $\alpha_T = 1 + \beta_T^2$, otherwise different formulas are obtained) [27–30],

$$\hat{\mathbf{P}}_{2D}^{-1}|\hat{\mathbf{P}}_{2D}\hat{\mathbf{A}}_{\parallel}| = \hat{a}_s \begin{pmatrix} \frac{\sqrt{1-\hat{M}^2}}{\hat{\beta}_T} & 0 & 0 & 0 \\ \frac{\hat{M}\hat{\alpha}_T\sqrt{1-\hat{M}^2}}{\hat{\beta}_T} & \hat{\beta}_T\sqrt{1-\hat{M}^2} & 0 & 0 \\ 0 & 0 & \hat{M} & 0 \\ 0 & 0 & 0 & \hat{M} \end{pmatrix};$$

$$\hat{\mathbf{P}}_{2D}^{-1}|\hat{\mathbf{P}}_{2D}\hat{\mathbf{A}}_{\perp}| = \hat{a}_s \begin{pmatrix} \frac{1}{\hat{\beta}_T} & 0 & 0 & 0 \\ \frac{M\hat{\alpha}_T}{\hat{\beta}_T} & 0 & 0 & 0 \\ 0 & 0 & \hat{\beta}_T & 0 \\ 0 & 0 & 0 & 0 \end{pmatrix}. \tag{69}$$

Note that the optimal value of β_T is M, which further simplifies the above formulas.

With $\mathbf{P}_{\mathrm{stag,streamwise}}(b_0 = 0)$, these matrices become

$$\hat{\mathbf{P}}_{2D}^{-1}|\hat{\mathbf{P}}_{2D}\hat{\mathbf{A}}_{\parallel}| = \hat{a}_s \begin{pmatrix} -\hat{M}\sqrt{1-\hat{M}^2} & -\frac{\sqrt{1+\hat{M}^2}}{\hat{M}^2\sqrt{1-\hat{M}^2}} & 0 & 0 \\ \frac{\sqrt{1+\hat{M}^2}}{\hat{M}^2\sqrt{1-\hat{M}^2}} & \hat{M}\sqrt{1-\hat{M}^2} & 0 & 0 \\ 0 & 0 & \hat{M} & 0 \\ 0 & 0 & 0 & \hat{M} \end{pmatrix};$$

$$\hat{\mathbf{P}}_{2D}^{-1}|\hat{\mathbf{P}}_{2D}\hat{\mathbf{A}}_{\perp}| = \hat{a}_s \begin{pmatrix} \frac{1}{\hat{M}} & 0 & 0 & 0 \\ 0 & 0 & 0 & 0 \\ 0 & 0 & \hat{M} & 0 \\ 0 & 0 & 0 & 0 \end{pmatrix}. \tag{70}$$

For the all purpose ζ–family preconditioner,

$$\hat{\mathbf{P}}_{2D}^{-1}|\hat{\mathbf{P}}_{2D}\hat{\mathbf{A}}_{\parallel}| = \hat{a}_s \begin{pmatrix} \frac{|\hat{M}^2-1|+1}{\hat{M}} - \frac{2\hat{\beta}(\zeta+1)}{\hat{M}(1+\hat{\beta})} & 1 & 0 & 0 \\ 1 - \frac{\hat{\beta}(\zeta+1)}{(1+\hat{\beta})} & \hat{M} & 0 & 0 \\ 0 & 0 & \hat{M} & 0 \\ 0 & 0 & 0 & \hat{M} \end{pmatrix};$$

$$\hat{\mathbf{P}}_{2D}^{-1}|\hat{\mathbf{P}}_{2D}\hat{\mathbf{A}}_{\perp}| = \hat{a}_s \begin{pmatrix} \frac{\hat{\beta}}{\hat{M}} & 0 & 0 & 0 \\ 0 & 0 & 0 & 0 \\ 0 & 0 & \frac{\hat{M}}{\hat{\beta}} & 0 \\ 0 & 0 & 0 & 0 \end{pmatrix}. \tag{71}$$

REFERENCES

1. S. R. Allmaras, *Analysis of Semi-implicit Preconditioners for Multigrid Solution of the 2-d Compressible Navier–Stokes Equations*, AIAA Paper 95-1651-CP, 1995.
2. P. Buelow, S. Venkateswaran, and C. L. Merkle, The effect of grid aspect ratio on convergence, in *AIAA 12th Computational Fluid Dynamics Conference, 1995*.
3. A. J. Chorin, A numerical method for solving incompressible viscous flow problems, *J. Comput. Phys.* **2** (1967).
4. D. L. Darmofal and P. J. Schmid, The importance of eigenvectors for local preconditioning of the Euler equations, *J. Comput. Phys.* **127**(2) (1996).
5. H. Deconinck and G. Degrez, Monotone shock-capturing cell vertex schemes for the Euler and Navier–Stokes equations on unstructured grids, in *Fifteenth International Conference on Numerical Methods in Fluid Mechanics* (Springer-Verlag, New York, 1996).
6. H. Deconinck, C. Hirsch, and J. Peuteman, Characteristic decomposition methods for the multidimensional Euler equations, in *Lectures Notes in Physics* (Springer-Verlag, New York/Berlin, 1987), Vol. 264.
7. A. G. Godfrey, *Topics on Spatially Accurate Methods and Preconditioning for the Navier–Stokes Equations with Finite-Rate Chemistry*, Ph.D. thesis, VPI & SU, 1992.
8. A. G. Godfrey, private communication, 1994.
9. A. G. Godfrey, *Steps Towards a Robust Preconditioning*, AIAA Paper 94-0520, 1994.
10. A. G. Godfrey, R. W. Walters, and B. van Leer, *Preconditioning for the Navier–Stokes Equations with Finite-Rate Chemistry*, AIAA Paper 93-0535, 1993.
11. S. K. Godunov, An interesting class of quasilinear systems, *Dokl. Akad. Nauk SSSR* **139**, 521 (1961).
12. P. D. Lax, Hyperbolic systems of conservation laws and the mathematical theory of shock waves, *Regional Conf. Ser. Appl. Math. SIAM* **11**, 521 (1973).
13. D. Lee, *Local Preconditioning of the Euler and the Navier–Stokes Equations*, Ph.D. Thesis, University of Michigan, 1996.
14. W.-T. Lee, *Local Preconditioning of the Euler Equations*, Ph.D. thesis, University of Michigan, 1991.

14a. D. Lee, The Design of Local Navier–Stokes Preconditioning for Compressible Flow, *J. Comput. Phys*. **144**, 460 (1998).

15. J. F. Lynn, *Multigrid Solution of the Euler Equations with Local Preconditioning*, Ph.D. thesis, University of Michigan, 1995.
16. C. L. Merkle and Y.-H. Choi, Computation of low-speed compressible flows with time-marching procedures, *Int. J. Numer. Methods Eng.* **25**, 293 (1988).

17. L. M. Mesaros, *Multi-Dimensional Fluctuation Splitting Schemes for the Euler Equations on Unstructured Grids*, Ph.D. thesis, University of Michigan, 1995.
18. L. M. Mesaros and P. L. Roe, *Multidimensional Fluctuation-Splitting Schemes Based on Decomposition Methods*, AIAA Paper 95-1699, 1995.
19. J.-D. Müller, *On Triangles and Flow*, Ph.D. thesis, University of Michigan, 1995.
20. H. Pailère, H. Deconinck, R. Struijs, P. L. Roe, L. M. Mesaros, and J.-D. Müller, *Computations of Inviscid Compressible Flows Using Fluctuation-Splitting on Triangular Meshes*, AIAA Paper 93-3301, 1993.
21. N. A. Pierce and M. B. Giles, *Preconditioning Compressible Flow Calculations on Stretched Meshes*, AIAA Paper 96-0889, 1996.
22. Y. Saad and M. H. Schultz, *GMRES: A Generalized Minimal Residual Algorithm for Solving Nonsymmetric Linear Systems*, Research Report YALEU/DCS/RR-254, Yale University Department of Computer Science, 1983.
23. S. P. Spekreijse, *Multigrid Solution of the Steady Euler Equations*, Ph.D. thesis, Technische Universiteit Delft (Centrum voor Wiskunde en Informatica (CWI), Amsterdam, 1987).
24. R. Struijs, H. Deconinck, and P. L. Roe, Fluctuation splitting for the 2-D Euler equations, in *Computational Fluid Dynamics* (Von Kármán Institute for Fluid Dynamics, Lecture Series 1991-01, 1991).
25. S. Ta'asan, *Canonical Forms of Multidimensional Inviscid Flows*, ICASE Report 93-34, 1993.
26. C.-H. Tai, *Acceleration Techniques for Explicit Euler Codes*, Ph.D. thesis, University of Michigan, 1990.
27. E. Turkel, *Acceleration to a Steady State for the Euler Equations*, ICASE Report 84-32, 1984.
28. E. Turkel, *Preconditioned Methods for Solving the Incompressible and Low Speed Compressible Equations*, ICASE Report 86-14, 1986.
29. E. Turkel, Preconditioned methods for solving the incompressible and low speed compressible equations, *J. Comput. Phys.* **72** (1987).
30. E. Turkel, A. Fiterman, and B. van Leer, *Preconditioning and the Limit to the Incompressible Flow Equations*, ICASE Report 93-42, 1993.
31. B. van Leer, W. T. Lee, and P. L. Roe, Characteristic time-stepping or local preconditioning of the Euler equations, in *AIAA 10th Computational Fluid Dynamics Conference, 1991*.
32. B. van Leer, L. Mesaros, C.-H. Tai, and E. Turkel, Local preconditioning in a stagnation point, in *12th AIAA Computational Fluid Dynamics Conference* (AIAA Report AIAA-95-1654-CP, 1995), p. 88.
33. S. Venkateswaran and C. L. Merkle, Analysis of time-derivative preconditioning for the navier-stokes equations, in *6th International Symposium on Computational Fluid Dynamics, 1995*.
34. H. Viviand, Pseudo-unsteady systems for steady inviscid flow calculations, in *Numerical Methods for the Euler Equations of Fluid Dynamics, 1985*.
35. L. B. Wigton, N. J. Yu, and D. P. Young, GMRES acceleration of computational fluid dynamics codes, in *AIAA 7th Computational Fluid Dynamics Conference, 1985*.